

EGG-WM--9041

DE91 001891

EGG-WM-9041

**OGRE/MOD1: A COMPUTER MODEL FOR PREDICTING OFF-GAS RELEASE  
FROM IN SITU VITRIFICATION MELTS**

Robert J. MacKinnon  
Vincent A. Mousseau

Published July 1990

EG&G Idaho, Inc.  
Idaho Falls, ID 83415

Prepared for the  
U. S. Department of Energy  
Idaho Operations Office  
Under DOE Contract No. DE-AC07-76ID01570

**MASTER**

*ds*  
DISTRIBUTION OF THIS DOCUMENT IS UNLIMITED

OGRE/MOD1: A COMPUTER MODEL FOR  
PREDICTING OFF-GAS RELEASE FROM  
IN SITU VITRIFICATION MELTS  
EGG-WM-9041

Approved By: *S. W. Merrill* Date: 9/17/90  
S. W. Merrill, Manager  
In Situ Vitrification

Prepared By: *Robert J. MacKinnon* Date: 9/14/90  
R. J. MacKinnon

Reviewed By: *D. L. Hagrman* Date: 9/14/90  
D. L. Hagrman  
Technical Reviewer

## ABSTRACT

The OGRE program is designed to compute off-gas release from In Situ Vitrification melt pools. This document describes the theoretical basis and computational algorithms used in the program. An outline of the computer program is described including presentation of an example user input deck. Two model problems are examined to verify the program and an example problem is given to demonstrate program usage.

## NOMENCLATURE

Symbol	Description of Symbol
$b_g$	mass of gas mixture per unit volume ( $\text{kg}/\text{m}^3$ )
$b_{n,L}$	mass of nth gas species in the Lth bubble size per unit volume ( $\text{kg}/\text{m}^3$ )
$D_m$	depth of melt/solid interface (m)
$D_s$	subsidence depth of the top melt surface (m)
$g$	gravitational acceleration ( $\text{m}/\text{s}^2$ )
$j_{gt}$	drift flux of the gas mixture (m/s)
$N$	number of chemical species
$P_c$	capillary pressure between the gas and melt (liquid) phases (Pascals)
$P_g$	pressure in the gas phase (Pascals)
$P_l$	pressure in the melt (liquid) phase (Pascals)
$Q_g$	gas mixture mass source rate per unit volume ( $\text{kg}/\text{m}^3\text{-s}$ )
$Q_{n,L}$	mass source rate of the nth species in the Lth bubble size per unit volume ( $\text{kg}/\text{m}^3\text{-s}$ )
$Q_o$	volumetric flow rate through an effective orifice ( $\text{m}^3/\text{s}$ )
$q_{gs}$	mass flux of gas at the subsidence surface ( $\text{kg}/\text{m}^2\text{-s}$ )
$q_g$	mass flux of gas at the melt/solid interface ( $\text{kg}/\text{m}^2\text{-s}$ )
$R$	gas constant ( $\text{m}^2/\text{s}^2\text{-K}$ )
$R_b$	effective bubble radius (m)
$\bar{S}$	average vertical gas velocity (m/s)
$S_o$	terminal rise velocity (m/s)
$S_L$	rise velocity of the size L bubble (m/s)

Superscripts

i	agglomeration exponent
n	time level

$T_l$	temperature of the liquid phase (K)
$V_b$	effective bubble volume ( $m^3$ )
$v_l$	vertical liquid velocity (m/s)
$We_{crit}$	Critical Weber number

### Greek

$\alpha$	volumetric concentration of gas (void fraction)
$\mu_l$	dynamic viscosity of the liquid (kg/m-s)
$\omega$	relaxation parameter
$\rho_g$	gas density ( $kg/m^3$ )
$\rho_l$	liquid density ( $kg/m^3$ )
$\sigma$	surface tension ( $kg/s^2$ )

### Subscripts

b	bubble
c	capillary
g	gas
$\infty$	terminal (steady state)
k	node point value
l	liquid
$\bar{L}$	average bubble size
m	melt
n	chemical species
0	initial
s	subsidence surface

## CONTENTS

1.	Introduction .....	1
2.	The Physical Model .....	2
2.1	Continuous Equations .....	4
2.2	Terminal Rise Velocity .....	7
2.3	Initial Bubble Size and Bubble Growth .....	8
2.4	Numerical Approximation .....	19
3.	Program Description .....	22
3.1	Overall Flow Chart .....	22
3.2	Organization and Description of Subroutines .....	24
3.3	Input .....	27
4.	Model Verification .....	31
4.1	Step Wave Test Problem .....	31
4.2	Rectangular Wave Test Problem .....	31
4.3	Example Application .....	32
4.4	Further Development .....	32

## FIGURES

2.1	Idealized Configuration of the ISV Melt Pool .....	3
2.2	Terminal Velocity of Air Bubbles in Distilled Water as a Function of Equivalent Bubble Radius .....	10
2.3	The Dependence of Initial Bubble Size on Pore Size .....	12
2.4	The Dependence of Initial Bubble Size on Gas Flow Rate .....	13
2.5	Effect of Gravity on Bubble Volume .....	14
2.6	Effect of Agglomeration on Bubble Volume .....	16
2.7	Combined Effects of Gravity and Agglomeration on Bubble Volume .....	17

2.8	The Dependence of Maximum Bubble Size and Rise Velocity .....	18
3.1	OGRE/MOD1 Top Level Flow Chart .....	23
3.2	OGRE/MOD1 Top Level Tree Diagram .....	28
4.1	Spatial Distribution of Void Fraction at $t = 0.5$ s for the Step Wave .....	35
4.2	Gas Release vs. Time for Step Wave Propagation .....	36
4.3	Spatial Distribution of Void Fraction at $t = 0.61$ s for the Rectangular Wave .....	37
4.4	Gas Release vs. Time for Rectangular Wave Propagation .....	38
4.5	Off-Gas Release Rate vs. Time for Combined Steady and Sudden Gas Influx .....	39
4.6	Total Gas Volume Released vs. Time for Combined Steady and Sudden Gas Influx .....	40

#### TABLES

2.1	Terminal Velocity of Single Gas Bubbles in the Melt Pool .....	9
3.1	Example Input Deck for OGRE/MOD1 .....	29
4.1	Preliminary Comments About Model Parameters .....	33



## 1. INTRODUCTION

OGRE is a computer model for simulating off-gas release from In Situ Vitrification (ISV) melt pools. This document describes OGRE's basic equations, auxiliary models, formulations of approximate equations, and the overall structure of the program. In the development of OGRE, an attempt has been made to approximate gas transport and release in an average sense rather than explicitly recognizing individual chemical species and multidimensional flow. To this end, the model approximates one-dimensional transport and release of a single phase gas mixture which rises through the melt as a collection of bubbles of equal "effective" size. The rise velocity of the gas mixture is described by the local gas concentration and terminal velocity of the "effective" bubbles. The effects of agglomeration, pressure and temperature variations on bubble growth are included.

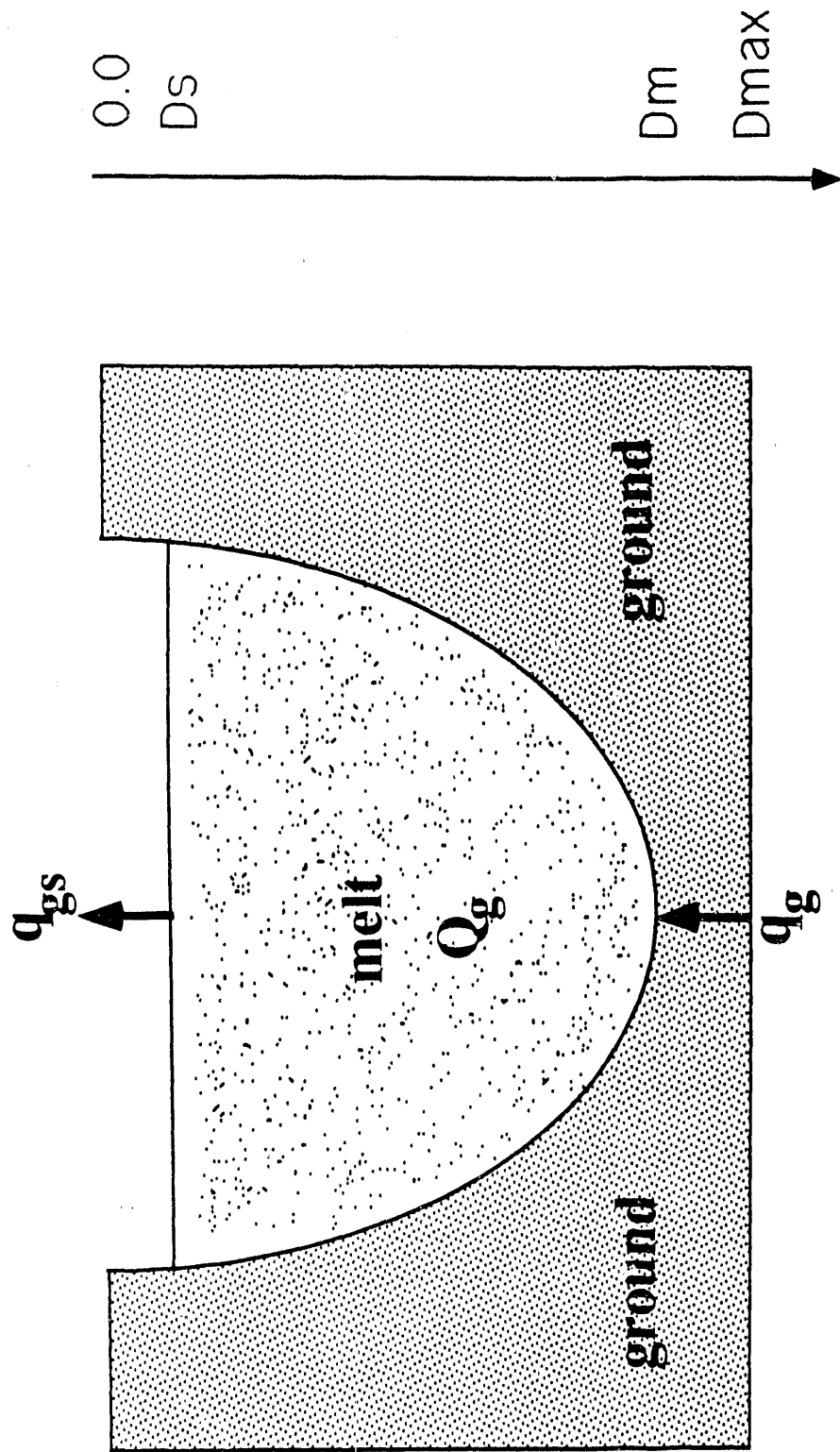
The organization of this report is as follows. In the next section the physical problem considered herein is described. The governing equations are then summarized as well as the set of auxiliary relations and boundary conditions needed to complete the mathematical statement of the problem. This section is followed by the approximate model for off-gas release. Included here are descriptions of the numerical discretization and solution schemes. In section 3 the overall structure of OGRE is described and an example input is given. Section 4 compares model solutions with exact solutions for two test problems. Finally, an example application is presented and comments regarding further development are given.

## 2. THE PHYSICAL MODEL

Consider the melt pool configuration shown in Figure 1. The system coordinate axis,  $x$ , decreases in the downward direction with  $x = 0$  at the ground surface,  $x = D_s$  at the melt subsidence surface, and  $x = D_m$  at the bottom of the melt pool. Gases enter the melt pool in the form of bubbles as a result of a boundary flux,  $q_g$ , at  $x = D_m$  and/or as a distributed source  $Q_g$ . These bubbles subsequently rise through the melt pool with a positive vertical velocity and are released at the surface,  $x = D_s$ , at a rate  $q_{gs}$  per unit surface area. The primary unknowns to be determined by the mathematical model are: the spatial and temporal distribution of gas in the melt, and the rate at which gases are released at the melt subsidence surface.

The major model assumptions are summarized as follows:

1. The transport of gas in the melt pool is primarily by bubble rise.
2. The range of bubble sizes entering the melt can be represented by a single "effective" bubble size.
3. The distribution of chemical species within the gas bubbles can be represented by a single gas mixture.
4. Horizontal melt velocities are negligible compared to vertical melt and bubble rise velocities.
5. Hold-up effects due to cold cap formation and shear effects due to melt pool and electrode boundaries can be neglected.
6. The bubbles are in thermal equilibrium with their surroundings.
7. No phase change.



2.1 Idealized Configuration of the ISV Melt Pool

## 2.1 Continuous Equations

The distribution of chemical species within the gas bubbles is given by<sup>1</sup>

$$\frac{\partial}{\partial t} b_{n,L} + \frac{\partial}{\partial x} (S_L b_{n,L}) - Q_{n,L} \quad \text{in } D_m \leq x \leq D_s \leq 0 \quad (2.1)$$

where

$b_{n,L}$  = mass of nth gas species in the Lth bubble size class per unit volume ( $\text{kg/m}^3$ )

$S_L$  = local average rise velocity of the Lth bubble size class (m/s)

$Q_{n,L}$  = mass source rate due to chemical reactions and vaporization ( $\text{kg/m}^3\text{-s}$ )

$D_s$  = subsidence depth of the top melt surface (m)

$D_m$  = depth of the melt/solid interface (m)

and n and L range over the number of species and bubble size classes, respectively. Equations (2.1) can be reduced to a single equation by considering a gas mixture which occupies a single effective bubble size class  $\bar{L}$ .

The mass of the gas mixture per unit volume in the  $\bar{L}$ th bubble size class is defined as

$$b_g = \sum_{n=1}^N b_{n,\bar{L}} \quad (2.2)$$

for N chemical species. Similarly, the mixture gas source term,  $Q_g$ , is

$$Q_g = \sum_{n=1}^N Q_{n,\Gamma} \quad (2.3)$$

To obtain the continuity equation for the gas mixture, equations (2.1) are summed over the N species

$$\frac{\partial}{\partial t} \sum_{n=1}^N b_{n,\Gamma} + \frac{\partial}{\partial x} \left[ \bar{S} \sum_{n=1}^N b_{n,\Gamma} \right] = \sum_{n=1}^N Q_{n,\Gamma} \quad \text{in } D_m \leq x < D_s \quad (2.4)$$

where  $\bar{S}$  is the average rise velocity of the gas mixture.

Introducing (2.2) and (2.3) into (2.4) yields

$$\frac{\partial}{\partial t} b_g + \frac{\partial}{\partial x} (\bar{S} b_g) = Q_g \quad \text{in } D_m \leq x \leq D_s \quad (2.5)$$

The solution to (2.5) gives the transient distribution of gas,  $b_g$ , in the melt. From this solution the flow rate (off-gas release rate) at the melt surface may be determined by simply evaluating  $\bar{S} b_g$  at the subsidence surface.

The initial condition for equation (2.5) is

$$b_g(x, 0) = \alpha_o \rho_{go} \quad , \quad D_m \leq x \leq D_s \quad (2.6)$$

where  $\alpha_o$  and  $\rho_{go}$  are initial gas concentration and density. The boundary condition at the melt/solid interface is

$$b_g = q_g / \bar{S} \quad x = D_m, t > 0 \quad (2.7)$$

where  $q_g$  is the mass flux of gas from the solid region into the melt. This mass flux is due to chemical reactions and vaporization in the solid region ahead of the melt front and is the primary source of gas.

The density of the gas mixture is given by the ideal gas law

$$\rho_g = \frac{P_g}{R T_l} \quad (2.8)$$

where  $P_g$  is gas pressure and  $T_l$  is melt temperature.  $P_g$  is equal to the sum of melt pressure,  $P_l$ , and capillary pressure  $P_c$ , that is

$$P_g = P_l + P_c = P_l + \frac{2\sigma}{R_b} \quad (2.9)$$

where  $\sigma$  denotes melt/gas interfacial surface tension,  $R_b$  is the effective bubble radius for bubble size class  $\bar{l}$ , and it is assumed that  $P_c$  may be approximated by Laplace's equation for mechanical equilibrium of a surface between two fluids.

The gas velocity,  $\bar{S}$ , is assumed to be a function of the volumetric concentration of gas. The volumetric concentration of gas,  $\alpha$ , is determined from the solution of (2.5) and equation (2.8) using the relationship

$$\alpha = b_g / \rho_g \quad (2.10)$$

For one-dimensional vertical bubbly flows without wall shear, the following equation has been found to correlate with a wide variety of data<sup>2</sup>

$$j_{gl} = S_\infty \alpha (1-\alpha)^i \quad (2.11)$$

where  $j_{gl}$  is the drift-flux,  $S_{\infty}$  is the terminal velocity of a single bubble of size  $R_b$ , and exponent  $i$  is determined experimentally. The drift flux can be rewritten in terms of the average mixture velocity as

$$j_{gl} = \alpha (1-\alpha) (\bar{S} - v_l) \quad (2.12)$$

where  $v_l$  is the local vertical liquid melt velocity.

The average gas velocity,  $\bar{S}$ , can now be written in terms of gas concentration,  $\alpha$ , and terminal velocity  $S_{\infty}$ . Setting (2.11) equal to (2.12) and solving for the average local vertical gas velocity yields

$$\bar{S} = S_{\infty} (1-\alpha)^{i-1} + v_l \quad (2.13)$$

Finally, the off-gas release at the top melt surface is given by

$$q_{gs} = b_g \bar{S} \quad x = D_s, t > 0 \quad (2.14)$$

Continuity equation (2.5) and initial and boundary conditions (2.6) and (2.7), along with equation of state (2.8), relations (2.9), (2.10), and (2.13), and off-gas flux equation (2.14) define the simplified off-gas release model.

## 2.2 Terminal Rise Velocity

The dependence of terminal rise velocity,  $S_{\infty}$ , of a single bubble on fluid properties is discussed in the In Situ Vitrification Model Development and Implementation Plan<sup>1</sup> and elsewhere.<sup>3</sup> Based on experimental measurements of gas bubbles in a variety of liquids, Peebles and Garber<sup>3</sup> developed a set of empirical relations for terminal rise velocity. These relations are used in this work and are presented in Table 2.1. The suitability of these correlations for ISV applications should be examined as experimental data become available.

For code verification purposes, these correlations are compared with experimental data<sup>4</sup> for an air water system in Figure 2.2. Results are computed using a uniform array of 1000 bubbles that range in size from 0.01 cm to 10 cm. Relevant properties are  $\mu_l = 0.001$  kg/m-s,  $\sigma = 0.0728$  kg/s<sup>2</sup>,  $\rho_l = 1000$  kg/m<sup>3</sup>,  $\rho_g = 1.16$  kg/m<sup>3</sup>, and  $g = 9.8$  m/s<sup>2</sup>. Figure 2.2 illustrates that computed velocities agree with the experimental data.

### 2.3 Initial Bubble Size and Bubble Growth

Gas is formed by high temperatures in the solid porous region ahead of the melt front. A portion of these gases enter the melt as bubbles. In this model the mechanism of bubble formation is assumed to be similar to bubble formation at the base of a liquid column caused by forcing gas through a series of orifices. For this case the initial bubble size is<sup>2</sup>

$$R_b(D_m) = \left[ \frac{\sigma R_p}{g(\rho_l - \rho_g)} \right]^{1/3} \quad (2.15a)$$

if  $R_b(D_m) > R_p$ , or

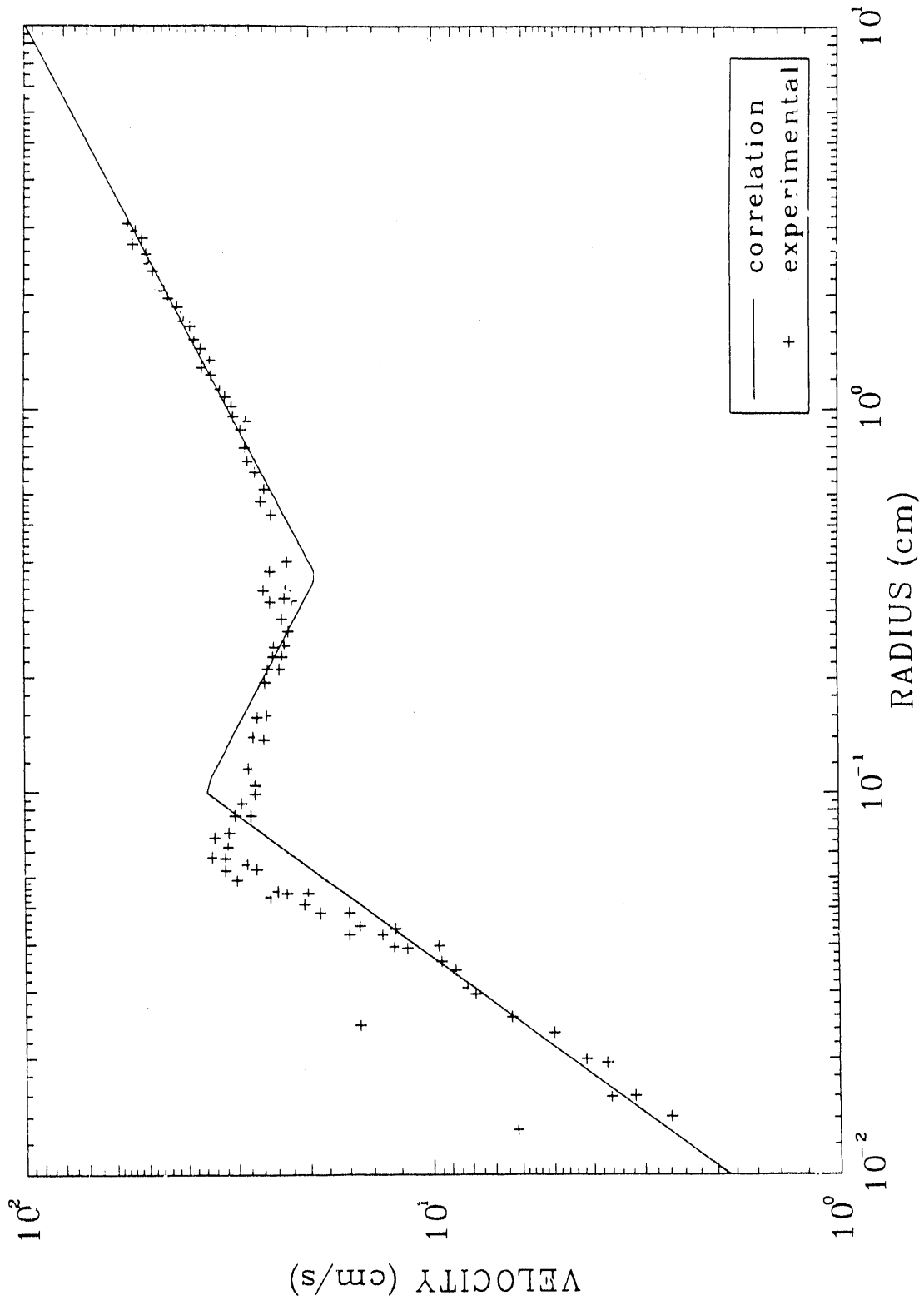
$$R_b(D_m) = .648 \left( \frac{Q_o^2}{g} \right)^{1/5} \quad (2.15b)$$

where  $\sigma$  is surface tension (kg/s<sup>2</sup>),  $\rho_l$  and  $\rho_g$  are liquid and gas densities in (kg/m<sup>3</sup>),  $g = 9.8$  m/s<sup>2</sup>,  $R_p$  is an orifice or pore throat radius and  $Q_o$  is the volumetric flow rate of gas through the orifice. For soil melts  $\rho_l \approx 2700$  kg/m<sup>3</sup>,  $\sigma$  might be approximately<sup>5</sup> .2371 kg/s<sup>2</sup>, and  $R_p = 0.25$  cm and  $Q_o = 0.5$  m<sup>3</sup>/min. Equations (2.15a) and (2.15b) yield initial bubble radii of 0.3 cm and 6.0 cm, respectively. The difference in the two computed bubble radii



Table 2.1. Terminal Velocity of Single Gas Bubbles in the Melt Pool

Terminal Velocity	Range of Applicability
$S_{\infty} = \frac{2R_b^2 \rho_l g}{9\mu_l}$	$R_b < 1.756 \left( \frac{\mu_l^2}{\rho_l^2 g} \right)^{1/3}$
$S_{\infty} = \frac{1}{3} g^{.76} \left( \frac{\rho_l}{\mu_l} \right)^{0.52} R_b^{1.28}$	$1.756 \left( \frac{\mu_l^2}{\rho_l^2 g} \right)^{1/3} < R_b < 2.194 \left( \frac{\sigma^{.5} \mu^{.52}}{\rho_l^{1.02} g^{.76}} \right)^{.56}$
$S_{\infty} = 1.35 \left( \frac{\sigma}{\rho_l R_b} \right)^{.5}$	$2.194 \left( \frac{\sigma^{.5} \mu^{.52}}{\rho_l^{1.02} g^{.76}} \right)^{.56} < R_b < 1.309 \left( \frac{\sigma}{\rho_l g} \right)^{.5}$
$S_{\infty} = 1.18 \left( \frac{g\sigma}{\rho_l} \right)^{.25}$	$1.309 \left( \frac{\sigma}{\rho_l g} \right)^{.5} < R_b < 1.392 \left( \frac{\sigma}{\rho_l g} \right)^{.5}$
$S_{\infty} = (g R_b)^{.5}$	$1.392 \left( \frac{\sigma}{\rho_l g} \right)^{.5} < R_b$



2.2 Terminal Velocity of Air Bubbles in Distilled Water as a Function of Equivalent Bubble Radius

indicates the present uncertainty in the size of bubbles entering the melt pool. Equation (2.15a) may be appropriate for the case of steady, slow gas production through small pores, whereas (2.15b) may be more appropriate for large gas surges into the melt. The dependence of bubble size on pore size and volumetric flow rate is shown in Figures 2.3 and 2.4.

If the bubbles which enter the melt are smaller than the maximum stable bubble size for the prevailing shear field, they will grow as they rise through the melt pool. This growth will occur for two main reasons:

1. Bubbles will agglomerate as they travel from the melt/solid interface to the melt surface.
2. A decrease in hydrostatic pressure and/or a change in melt temperature occurs as the bubble travels upward.

If mass does not enter or leave a bubble the growth as it rises is given by the ideal gas law

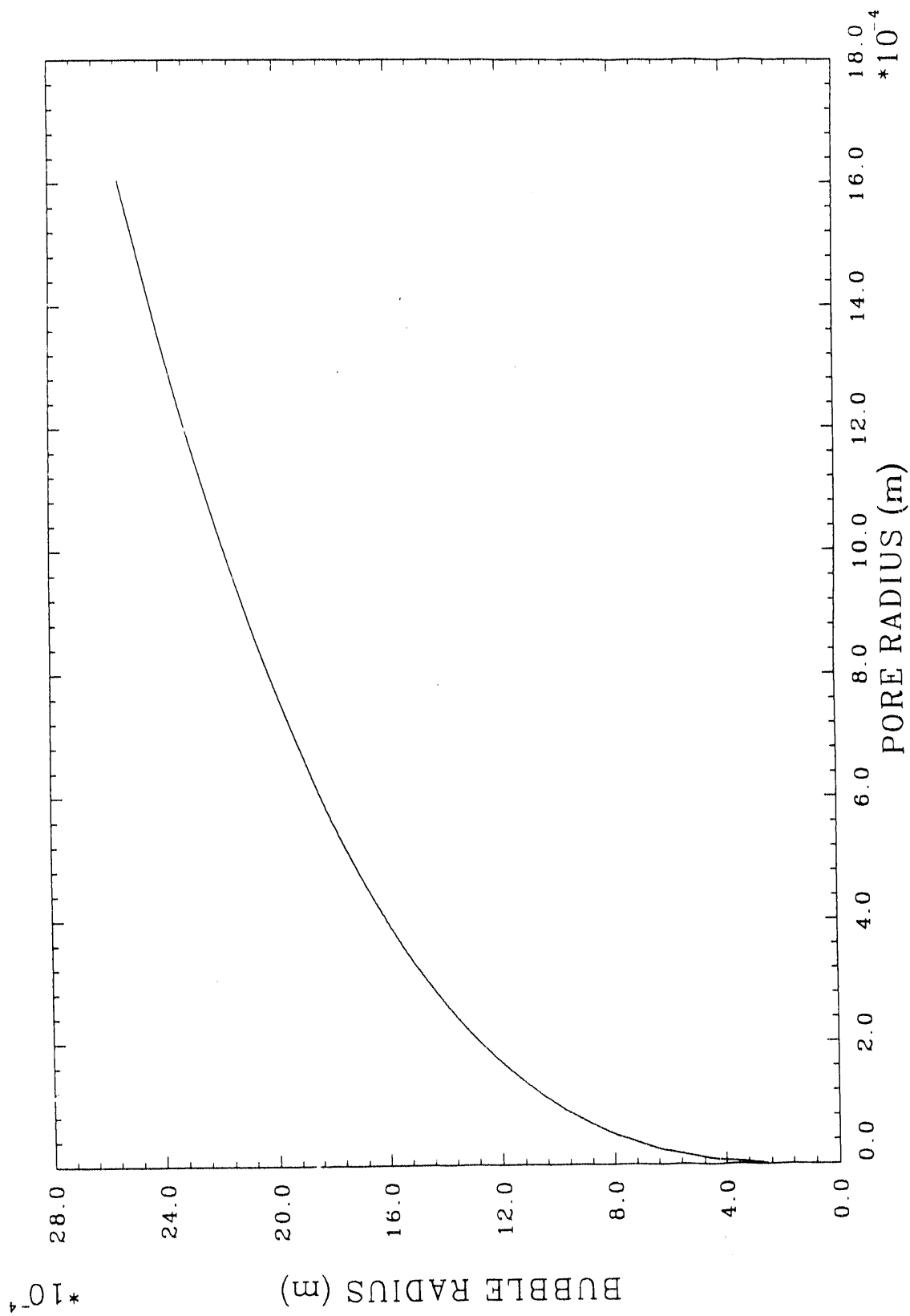
$$\frac{P_g(D_m) V_b(D_m)}{T_l(D_m)} = P_g(x) \frac{V_b(x)}{T_l(x)}, \quad D_m \leq x \leq D_s \quad (2.16)$$

where  $V_b$  is bubble volume. The change in bubble volume is therefore

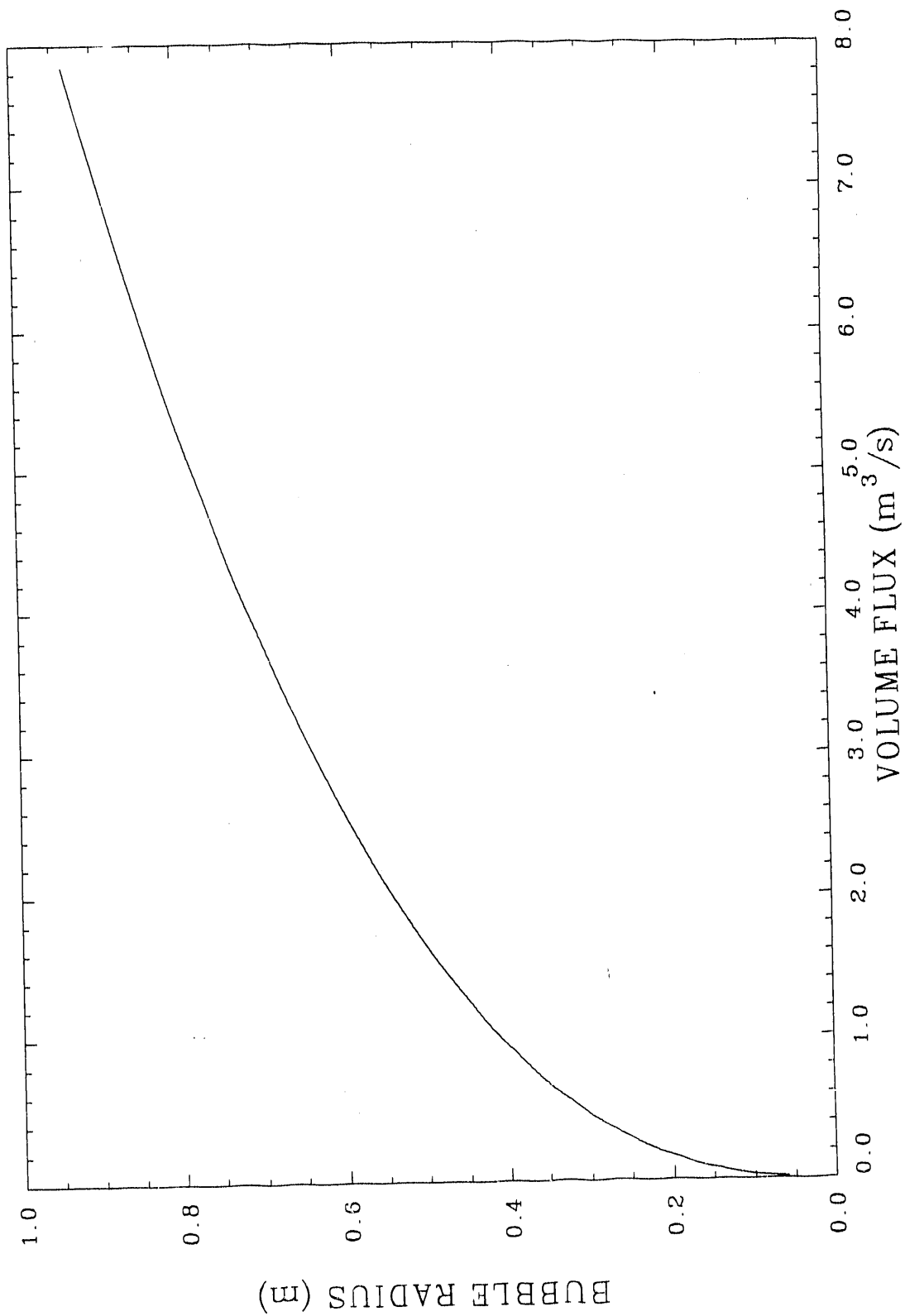
$$\Delta V_b(x) = \frac{T_m(x) P_g(D_m) V_b(D_m)}{T_m(D_m) P_g(x)} - V_b(D_m) \quad (2.17)$$

A plot of bubble volume as a result of pressure difference due to gravity is shown in Figure 2.5.

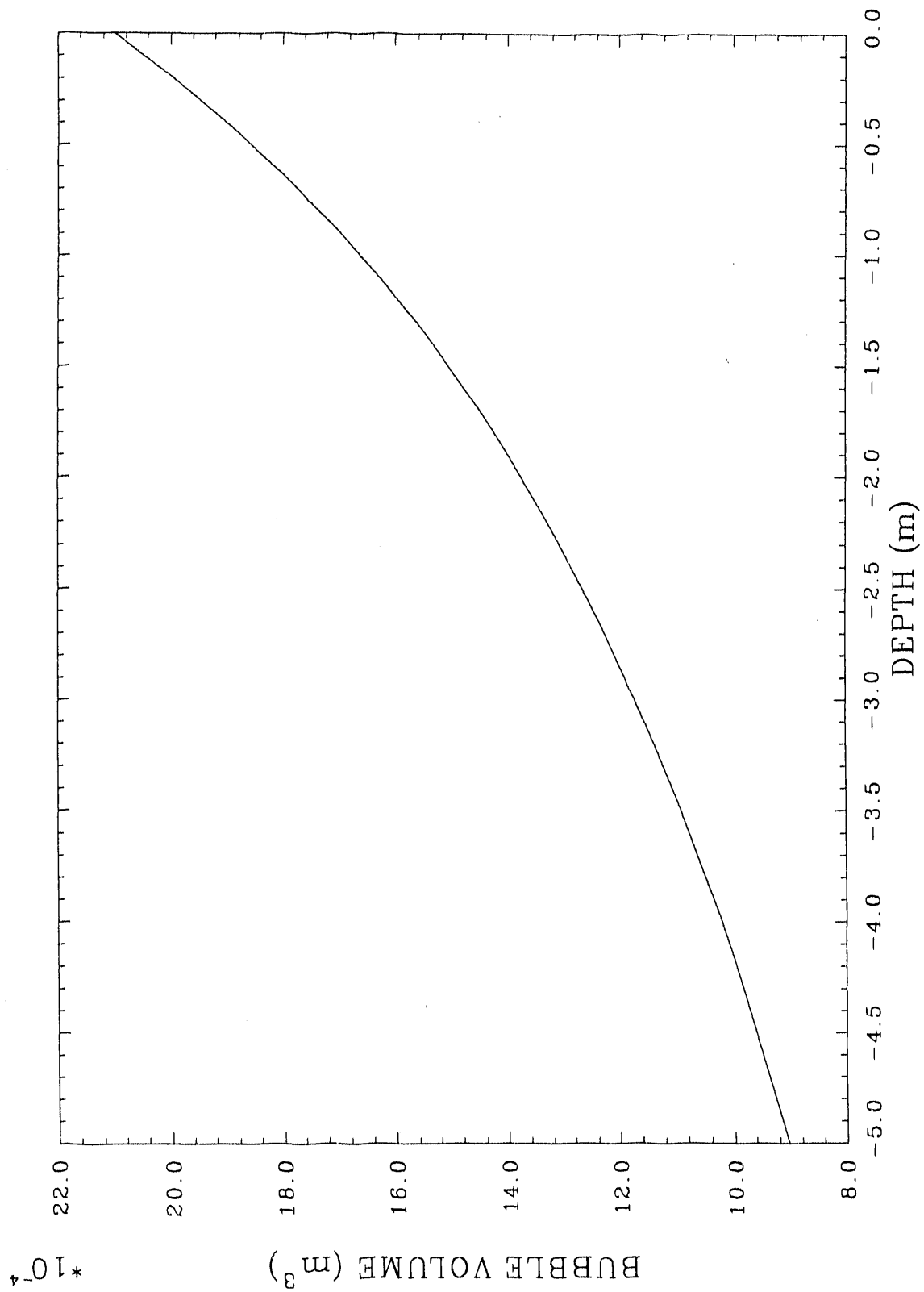
The agglomeration process is represented by a simple empirical power law relationship



2.3 The Dependence of Initial Bubble Size on Pore Size



2.4 The Dependence of Initial Bubble Size of Gas Flow Rate



2.5 Effect of Gravity on Bubble Volume

$$V_{ba}(x) = \left[ 1 + a \left( 1 - (x - D_s) / (D_m - D_s) \right)^b \right] V_b(D_m), \quad D_m \leq x \leq D_s \quad (2.18)$$

where coefficient  $a$  and exponent  $b$  are determined experimentally. A plot of bubble volume change due to agglomeration, for the case  $a=b=1$ , is shown in Figure 2.6.

The net bubble volume is found by combining (2.17) and (2.13), that is

$$V_b(x) = V_{ba}(x) + \Delta V_b \quad (2.19)$$

or

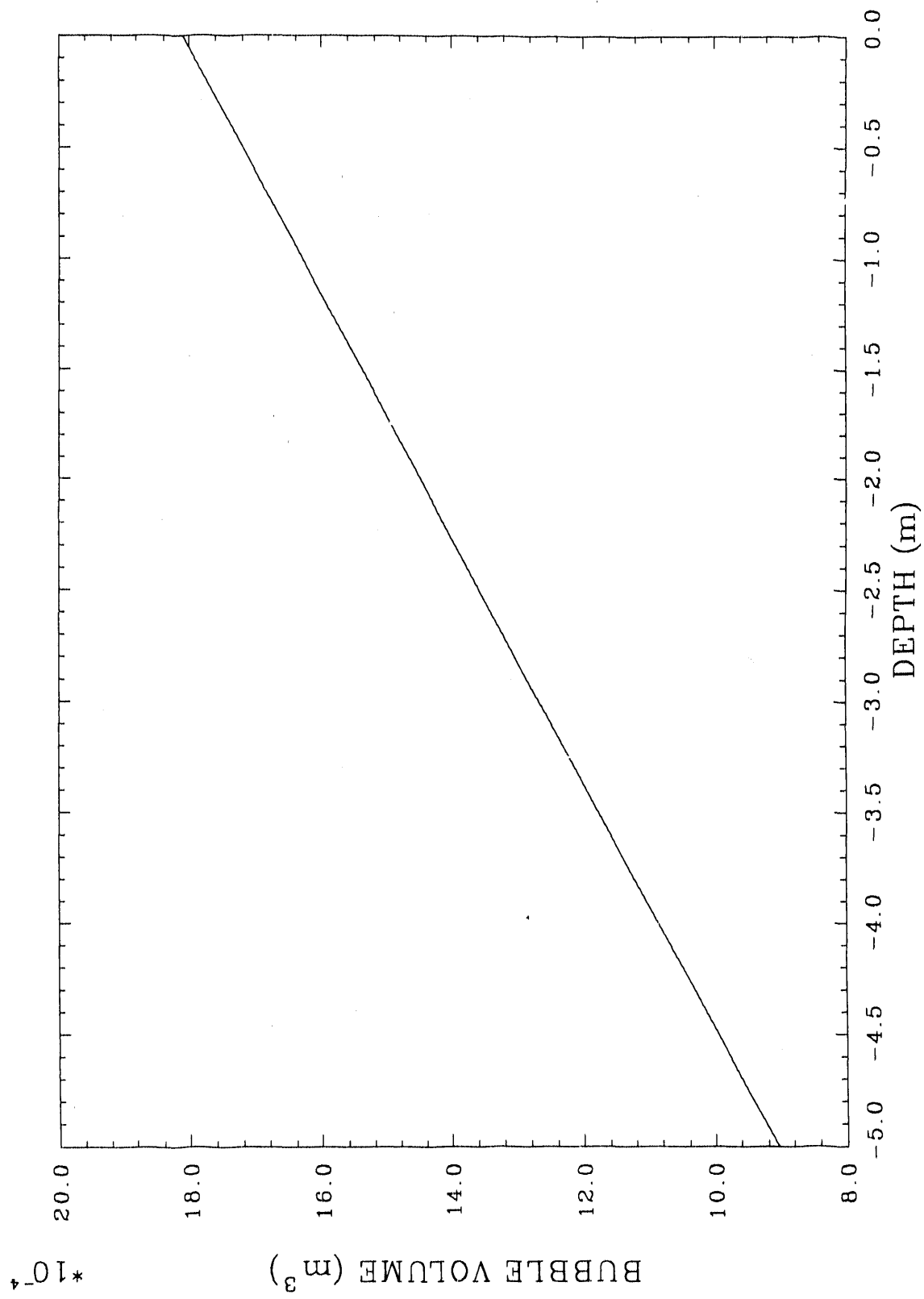
$$R_b = \left[ \frac{3}{4\pi} [V_{ba}(x) + \Delta V_b] \right]^{1/3} \quad (2.20)$$

The growth of a bubble due to both agglomeration and gravity effects is shown in Figure 2.7.

Gas bubbles rising through the melt cannot grow to be arbitrarily large. Eventually, a growing bubble will become unstable and break apart. This maximum bubble size is estimated by using a suitably chosen critical Weber number  $We_{crit}$ , that is

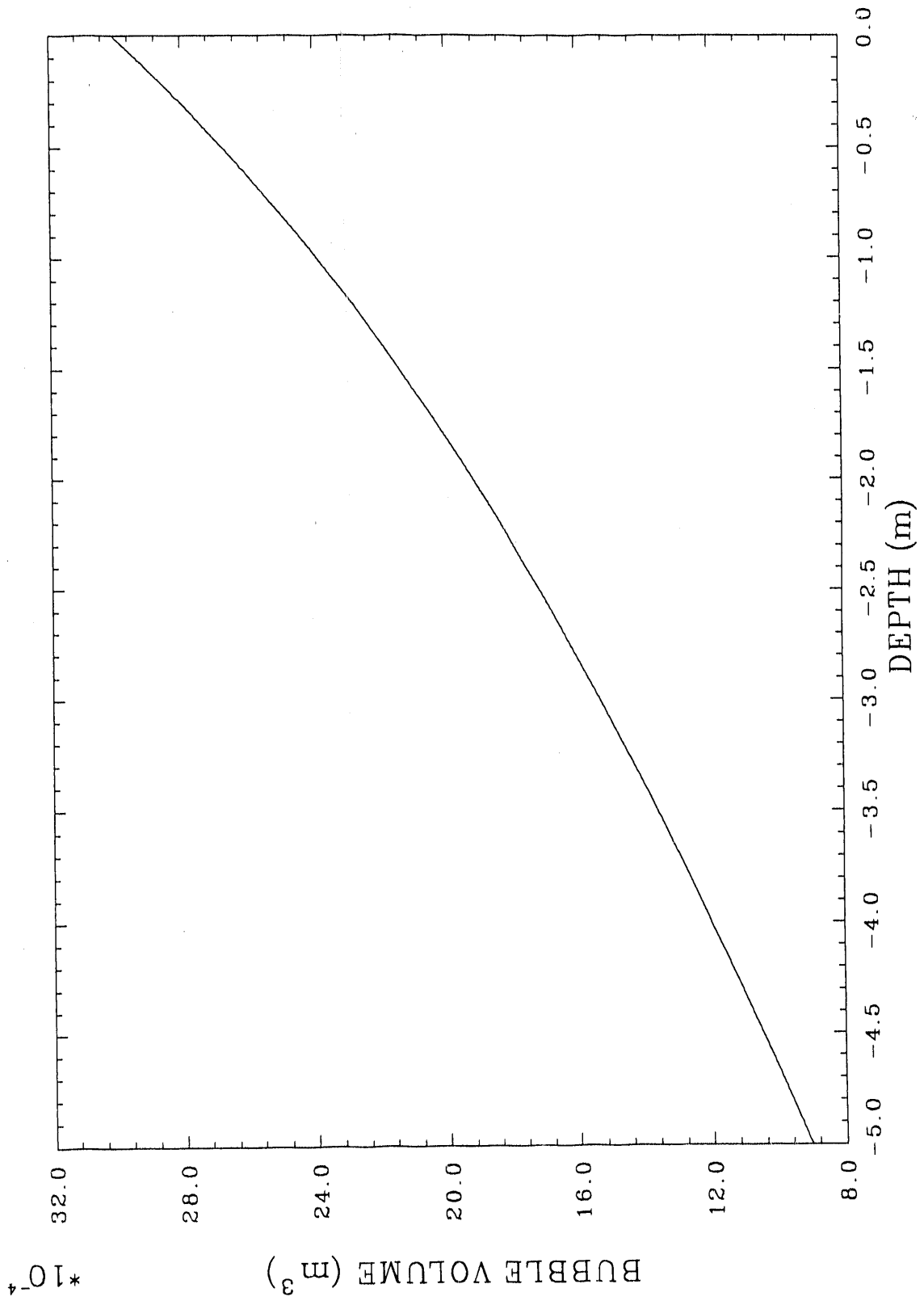
$$R_{bmax} = \frac{\sigma We_{crit}}{2 \rho_l (\bar{S} - V_l)^2} \quad (2.21)$$

Before representative values of  $R_{bmax}$  can be computed from (2.21), the magnitude of  $We_{crit}$  for ISV melts must be determined. For reference, typical values for non-viscous liquids such as water range from 7 to 12.<sup>6</sup> The dependence of stable bubble radius on bubble velocity for  $We_{crit} = 10$  is shown in Figure 2.8.

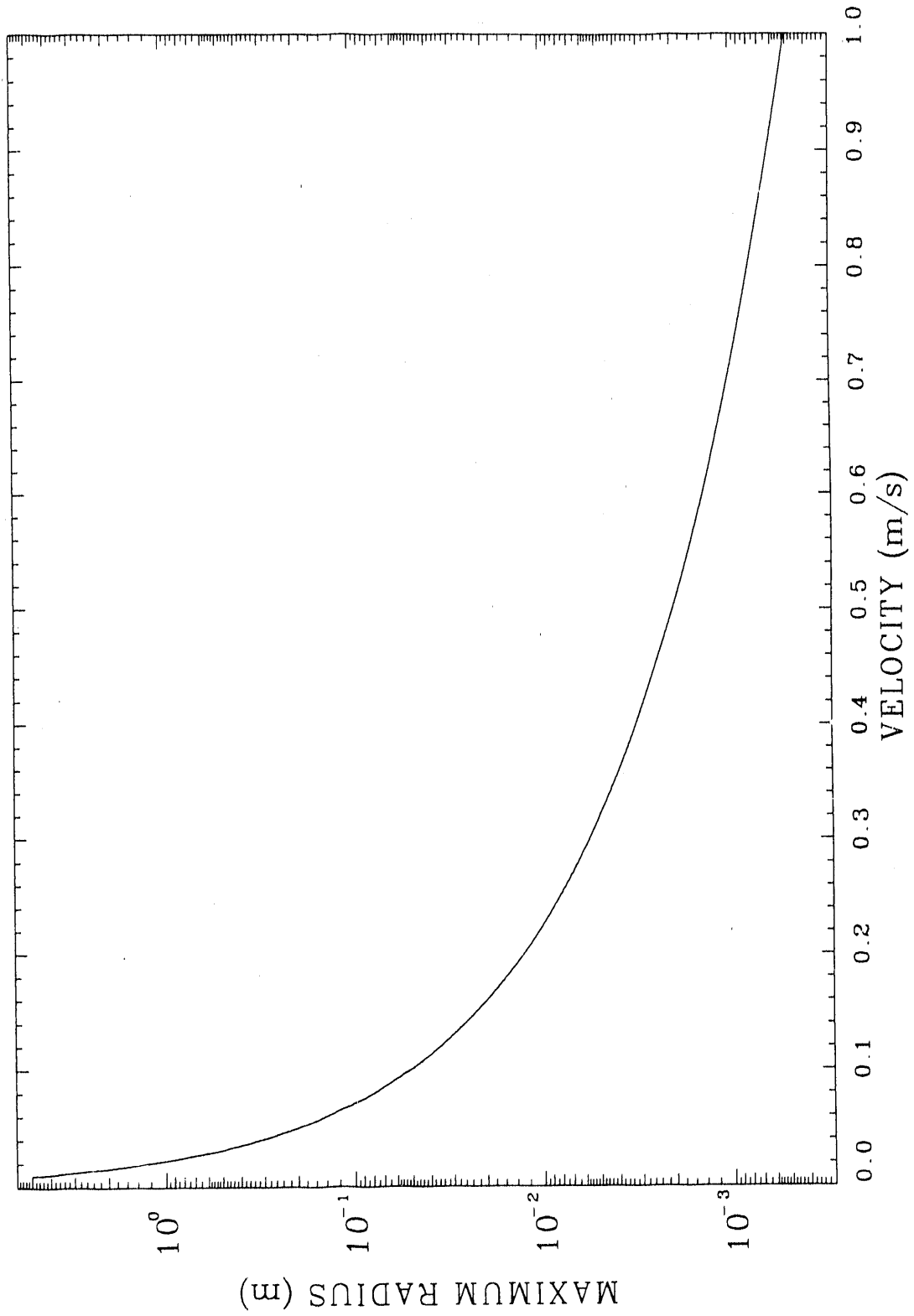


2.6 Effect of Agglomeration on Bubble Volume





2.7 Combined Effects of Gravity and Agglomeration on Bubble Volume



2.8 The dependence of Maximum Bubble Size and Rise Velocity

## 2.4 Numerical Approximation

A standard forward-time first-order upwind finite difference approximation to (2.5) is

$$\frac{b_{gk}^{n+1} - b_{gk}^n}{\Delta t} + \frac{\bar{S}_k^{n+1} b_{gk}^n - \bar{S}_{k+1}^{n+1} b_{gk+1}^n}{\Delta x} = Q_{gk}^n \text{ in } D_{\max} \leq D_m \leq x \leq D_s \leq 0 \quad (2.22)$$

where we have used conventional differencing notation

$$b_{gk}^n = b_g(k\Delta x, n\Delta t) \quad (2.23)$$

$k_{\max}$  grid spacings of length  $\Delta x = D_{\max}/k_{\max}$  are used on the interval  $D_{\max} \leq x \leq 0$  where  $D_{\max}$  is the maximum melt depth. The grid spacing in time is  $\Delta t$ , and at grid points  $(-k\Delta x, n\Delta t)$ ,  $k, n = 0, 1, 2, \dots$ , the function  $b_{gk}^n$  is the discrete finite difference approximation to the continuous function  $b_g$ . Remark: Computational cells in regions  $D_{\max} < x < D_m$  and  $D_s < x < 0$  are considered "inactive" and cells in region  $D_m \leq x \leq D_s$  are "active".

The initial and boundary conditions are

$$b_g(k\Delta x, 0) = \alpha_o \rho_o, \quad 0 \leq k \leq k_{\max} \quad (2.24)$$

and

$$q_g = b_g \bar{S}, \quad x = D_m, \quad t > 0 \quad (2.25)$$

Remarks: In general, the melt/solid interface will be located within a computational cell. In practice, boundary condition (2.25) is applied at the bottom boundary of the cell containing the interface.

An alternative representation of gas influx to the melt can be obtained by setting  $b_g = 0$  in the first inactive cell below the melt/solid interface

and applying an appropriate mass source  $Q_g$  in the active cell containing the interface.

The off-gas release at the subsidence surface is determined by evaluating (2.22) in the inactive cell at node  $k$  preceding the first active cell at node  $k+1$ . Setting  $b_{gk}^n = Q_{gk}^n = 0$  and solving for  $b_{gk+1}^{n+1} S_{gk+1}$ , the off-gas flux is given by

$$Q_{gs}^{n+1} = b_{gk+1}^{n+1} \bar{S}_{k+1}^{n+1} - \frac{\Delta x}{\Delta t} b_{gk}^{n+1} \quad (2.26)$$

The solution to (2.22) is stable for a Courant time step limit of

$$\bar{S}_k \frac{\Delta t}{\Delta x} \leq 1, \quad 0 \leq k \leq k_{\max} \quad (2.27)$$

The approximate gas density is found from (2.8)

$$\rho_{gk}^n = \frac{P_{gk}^n}{RT_{lk}^n} \quad (2.28)$$

where  $T_{lk}^n$  and  $P_{gk}^n$  are nodal temperatures and pressures.

The approximate void fraction  $\alpha$  is, from (2.10)

$$\alpha_k^n = \rho_{gk}^n / b_{gk}^n \quad (2.29)$$

Therefore, from (2.13), the approximate gas velocity at time  $n+1$  is

$$S_k^{n+1} = S_{\omega k}^{n+1} (1 - \alpha_k^n)^{i-1} + v_{lk}^n \quad (2.30)$$

The terminal velocity,  $S_{\omega k}^{n+1}$  in (2.30) is computed as follows. First the equivalent bubble volume at time  $n+1$  is calculated using (2.19) and under relaxation, that is

$$V_b^{n+1}(x) = (1-\omega) V_b^n(x) + \omega [V_{ba}(x) + \Delta V_b(x)] \quad (2.31)$$

for  $0 \leq \omega \leq 1$ . Hence, the corresponding equivalent bubble radii are

$$R_{bk}^{n+1} = \left[ \frac{3}{4\pi} V_{bk}^{n+1} \right]^{1/3} \quad (2.32)$$

These values of  $R_{bk}^{n+1}$ , and the correlations given in Table 1, are then used to compute terminal velocity  $S_{\omega k}^{n+1}$ .

The solution procedure, for a typical time step  $\Delta t$ , can be summarized as follows:

1. At the current time level  $n$ , compute bubble sizes for time level  $n+1$  using equations (2.15a), (2.15b), (2.21), and (2.31).
2. Using bubble sizes from 1, compute terminal velocities and average gas velocities at time level  $n+1$  from correlations in Table 1 and equation (2.30).
3. Solve continuity equation (2.22) for  $b_{gk}^{n+1}$ , and determine  $\alpha_k^{n+1}$  and  $\rho_{gk}^{n+1}$  using equations (2.28) and (2.29).
4. Compute gas release at the subsidence surface by evaluating equation (2.26).
5. If the required number of time steps has been performed then computation is terminated, otherwise steps 1-4 are repeated.

### 3. PROGRAM DESCRIPTION

The model developed in the previous section is incorporated into a FORTRAN program called OGRE. In the following sections a general description of the program is given.

#### 3.1 Overall Flow Chart

The overall structure of the computer code is shown in the flow chart presented in Figure 3.1. The major steps of the program are as follows:

- The simulation begins by reading input values, initializing all variables to their time zero values, and defining the computational grid. The subroutine SETUP is the main routine for initialization.
- After completion of initialization, subroutine BUBSIZ is called to compute the size of the bubbles as they enter the melt and travel upwards to the melt surface. Bubble sizes are then used to compute bubble velocities in subroutine MOMTUM.
- Subroutine CNTNTY is then called, boundary conditions are set and the continuity equation is solved for the spatial distribution of the mass per unit volume,  $b_g$ , at the new time. Solution  $b_g$  is then used to compute void fraction, gas density, and off-gas release.
- If the required number of time steps have been performed then computation is terminated. Otherwise old time values are updated and execution continues for the next time step.

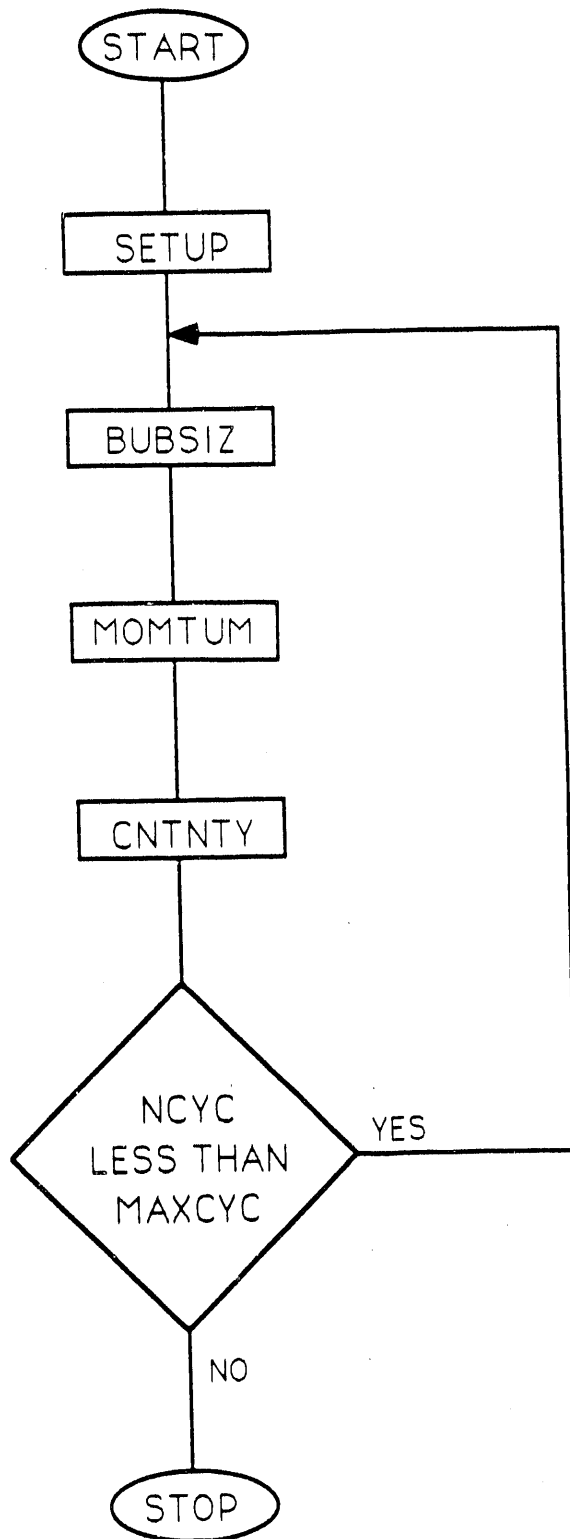


Figure 3.1. OGRE/MOD1 Top Level Flow Chart.

### 3.2 Organization and Description of Subroutines

OGRE is written in subroutine form such that each subroutine performs a separate logical task. The diagram in Figure 3.2 shows the organization of the subroutines in OGRE. Subroutine names have been selected to indicate the function that each routine performs, and these are arranged alphabetically. The following list gives a brief description of the functions performed by each subroutine.

1. AGGLOM (AGGLOMeration)

This subroutine computes the change in volume associated with agglomeration and other effects.

2. BCCNTY (Boundary Conditions CoNTinuity)

This subroutine sets the boundary conditions for the continuity equation.

3. BCMOM (Boundary Conditions MOMentum)

This subroutine sets the boundary conditions for the momentum equation.

4. BRAKUP (BReAK UP)

This subroutine sets the maximum bubble size based on the critical Weber number, and resets all volumes greater to the maximum value.

5. BUBSIZ (BUBble SIZE)

This subroutine computes the size of the bubbles.

6. CLOSFL (CLOSe File)

This subroutine closes the input and output files before the transient is terminated.

7. CNTNTY (CoNTiNuiTY)

This subroutine computes the continuity equation for the void.



8. CONVEC (CONVEction)

This subroutine computes the convection of the bubbles.

9. INIT (INITial)

This block data initializes all constants in the code, all input numbers that are seldom changed, and all time zero values that are never changed.

10. INITIAL (INITiALize)

This subroutine initializes the variables to their time zero values.

11. INITBB (INITialize BuBbles)

This subroutine initializes the bubble variables to their time zero values.

12. MONTUM (MOMentUM)

This subroutine computes the bubble velocity.

13. NEWTIM (NEW TIME)

This subroutine copies the new time values into the old time values in preparation for the next time step.

14. OGRE (Off-Gas RElease)

This program simulates off-gas release problem from an ISV melt pool.

15. OPENFL (OPEN FiLe)

This subroutine opens the input and output files needed for the code.

16. ORFICE (ORiFICE)

This subroutine computes the bubble size at the melt front based on orifice theory.

17. OUTPUT (OUTPUT)

This subroutine writes out the numerical data.

18. PRSHED (PReSsure HEaD)

This subroutine initializes the pressure head in the melt due to gravity.

19. REMASS (REmove MASS)

This subroutine removes the void from the top cell.

20. RESTRT (REStArT)

This subroutine reads the restart file Restart and initializes the code to the restart time (currently not active).

21. RINPUT (Read INPUT)

This subroutine reads the input values from the input deck in the file Ogre.inp.

22. SETUP (SET UP)

This subroutine reads the input values and the initializes the variables to their time zero values.

23. STATE (STATE)

This subroutine computes the density of the bubbles based on the ideal gas law with the gas constant chosen for air.

24. TIMPLT (TIME PLoT)

This subroutine outputs the data needed to make the time dependant plots.

25. TMPGRD (TEMPerature GRaDient)

This subroutine initializes the temperature gradient in the melt pool.

26. TRANS (TRANSient)

This subroutine controls when the transient ends and calls all of the subroutines that advance the bubbles one time step.

27. VNFNTY (Velocity INFINiTY)

This subroutine computes the steady state velocity of the bubbles.

### 3.3 Input

The units used in OGRE input are meter, kilogram, second, and Kelvins. Numerical values are entered in a free field format. An example data input deck is given in Table 3.1. A complete program variable dictionary is given in the Appendix.

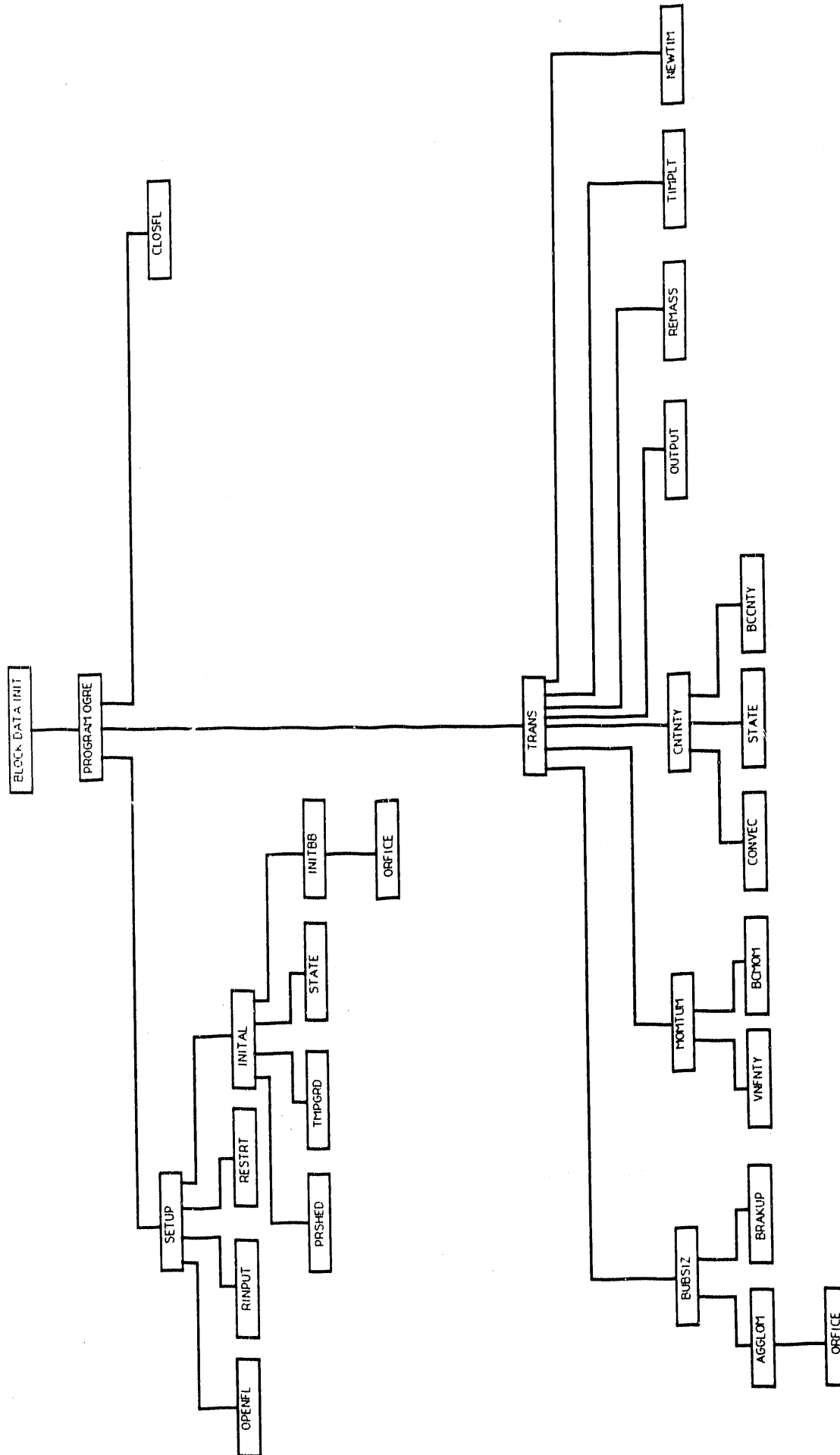


Table 3.1. Example Input Deck for OGRE/MOD1

```

'c'
'c'
'c'
100
3.00d-2
1.0d+1
100000
101
9.8d+0
1.0d-2
51
1
'c'
'c'
'c'
5.00d-3
100
10
1
1
1
10000
-1
'c'
'c'
'c'
1000.0d+0
300.0d+0
2.83d-4
0.0679d+0
'c'
'c'
'c'
1.0d-2
10.0d+0
1.0d+0
0.0d+0
3.0d+0
'c'
'c'
'c'
0.0d+0
1.0d-3
0.0d+0
'c'

```

GEOMETRY'

- \* ncells - number of real cells in the simulation
- \* dx - cell length
- \* diamc - diameter of the control volume (m)
- \* nhiac0 - the initial highest active cell
- \* lwact0 - the initial lowest active cell
- \* grav - acceleration due to gravity ( $m^2/s$ )
- \* radpor - radius of pores in front of the melt (m)
- \* ntdpcl - cell number for TDP data output
- \* nclskp - # of cells between surface plot output

TIME CONTROL'

- \* dt - time step (s)
- \* maxcyc - maximum number of time steps
- \* nprint - number of cycles between printed output
- \* nplot - number of cycles between plotting output
- \* ncycsb - the # cyc. before the surface moves 1 cell
- \* ncycft - the # cyc. before the front moves 1 cell
- \* ndbstt - cycle number to start debug output
- \* ndbstp - cycle number to stop debug output

FLUID PROPERTIES'

- \* rhof0 - the density of the melt pool ( $kg/m^3$ )
- \* t0 - the temperature of the melt pool ( $^{\circ}K$ )
- \* viscf0 - the viscosity of the melt pool ( $kg/m-s$ )
- \* sigf0 - the surface tension of the melt pool ( $kg/s^2$ )

CORRELATION COEFFICIENTS AND POWERS'

- \* timcon - the time for bubble volume change (s)
- \* wecrit - the critical weber number
- \* powagg - the power that sets the agglom curve.
- \* grwfrt - the bubble agglom growth fraction.
- \* power - wallis (4.14) n

INITIALIZATIONS'

- \* void0 - initial void fraction
- \* volb0 - initial average bubble volume ( $m^3$ )
- \* vbss0 - initial bubble velocity (m/s)

Table 3.1. (Continued)

---

'c	INFLOW CONDITIONS'
'c'	
3	* ncelin - cell to inject void at
0.00d+0	* voidin - amount of void to inject
10000	* ncycin - cycle number to inject void on
100000	* nsttgm - cycle to start gas inflow
50	* nstpgm - cycle to stop gas inflow
1.0d+1	* gamfrr - the void source at the front
1.0d-1	* vbbs - bubble velocity at the melt front
1.0d-3	* voidbc - void fraction at the melt front
'c'	
'c'	CODE FLAGS'
'c'	
1	* nbub0 - bub init flag (1) uniform (0) gradient
1	* ncvbss - bub vel flag (1) computed (0) vbinp
1.0d+0	* vbinp - bubble terminal velocity (m/s)
0	* norfis - orifice flag (1) computed (0) radbt0
1.0d-0	* radbt0 - bubble radius at melt bottom (m)
1	* nsorce - void source flag (1) cell (0) flux

## 4. MODEL VERIFICATION

Two model test problems and an example application problem are presented in this section. The test problems compare exact solutions, for step and rectangular wave propagation, with model solutions that are computed on successively refined time and space grids. The following sequence of grids are used:  $(\Delta x, \Delta t) = (1/9, 1/36)$ ,  $(1/81, 1/324)$ , and  $(1/729, 1/2916)$ . Following the two test problems, an example application is presented which simulates off-gas release for the condition of combined steady and sudden gas influx into the melt pool.

### 4.1 Step Wave Test Problem

This problem uses the following initial and boundary conditions:  $b_g(x,0) = 0$ ,  $-1 < x < 0$ ,  $b_g(-1,t) = 1.0 \text{ kg/m}^3$ ,  $t > 0$ . Parameters of interest include  $\bar{S} = 1.0 \text{ m/s}$  and  $\rho_g = 1 \text{ kg/m}^3$ . The distribution of void fraction at  $t = 0.5 \text{ s}$  and off-gas release rates at  $x = 0$  are shown in Figures 4.1 and 4.2. The first-order upwind scheme employed in OGRE produces artificial numerical diffusion and consequently coarse grid solutions suffer from inaccuracies as shown in Figures 4.1 and 4.2. However, results indicate that model solutions correctly converge toward the exact solution for successively refined grids.

### 4.2 Rectangular Wave Test Problem

This problem uses the following initial and boundary conditions:  $b_g(x,0) = 0$ ,  $-1 < x < 0$ ,  $b_g(-1,t) = 1 \text{ kg/m}^3$ ,  $0 < t < 2/9 \text{ s}$ . The distribution of void fraction at  $t = 0.61 \text{ s}$  and off-gas release rates at  $x = 0$  are shown in Figures 4.3 and 4.4. Again, results are similar to those of the previous problem and model solutions correctly converge toward the exact solutions for successively refined grids.

### 4.3 Example Application

This example problem consists of determining off-gas release for the following scenario. Gas enters the ISV melt at a steady rate,  $q_g = 0.008 \text{ kg/m}^2\text{-s}$ , and suddenly, at  $t = 10 \text{ s}$ , additional gas is released in the melt,  $Q_g = 1.0 \text{ kg/m}^3\text{-s}$ , for 1 s. The corresponding initial and boundary conditions are:  $b_g(x,0) = 0$ ,  $-5\text{m} < x < 0$ , and  $q_g(-5,t) = 0.008 \text{ kg/m}^2\text{-s}$ ,  $t > 0$ . The source term is  $Q_g(-5,t) = 1.0 \text{ kg/m}^3\text{-s}$ ,  $10 \text{ s} < t < 11 \text{ s}$ . Calculations are performed with  $\rho_{go} = .54 \text{ kg/m}^3$ , agglomeration parameter  $a = 0$ , and  $(\Delta x, \Delta t) = (.05\text{m}, .02\text{s})$ . Plots of off-gas release and total off-gas volume are shown in Figures 4.5 and 4.6. Note the sharp increase in off-gas release rate as the gas pulse reaches the surface.

### 4.4 Further Development

The current version of OGRE is a simplified, fast-running computer model for calculating off-gas release during In Situ Vitrification. Further development of this model will be guided by parametric studies and ISV test results that will be obtained in the remainder of FY 90 and FY 91. Results of these parametric studies and test analyses will be reported in two documents to be published in FY 1990.<sup>7,8</sup>

Table 4.1 is a preliminary list of parameters that need to be investigated. Materials, properties, boundary conditions, and model assumptions are included along with related comments. This table is presented here to stimulate discussion before the parametric studies<sup>7</sup> are completed.



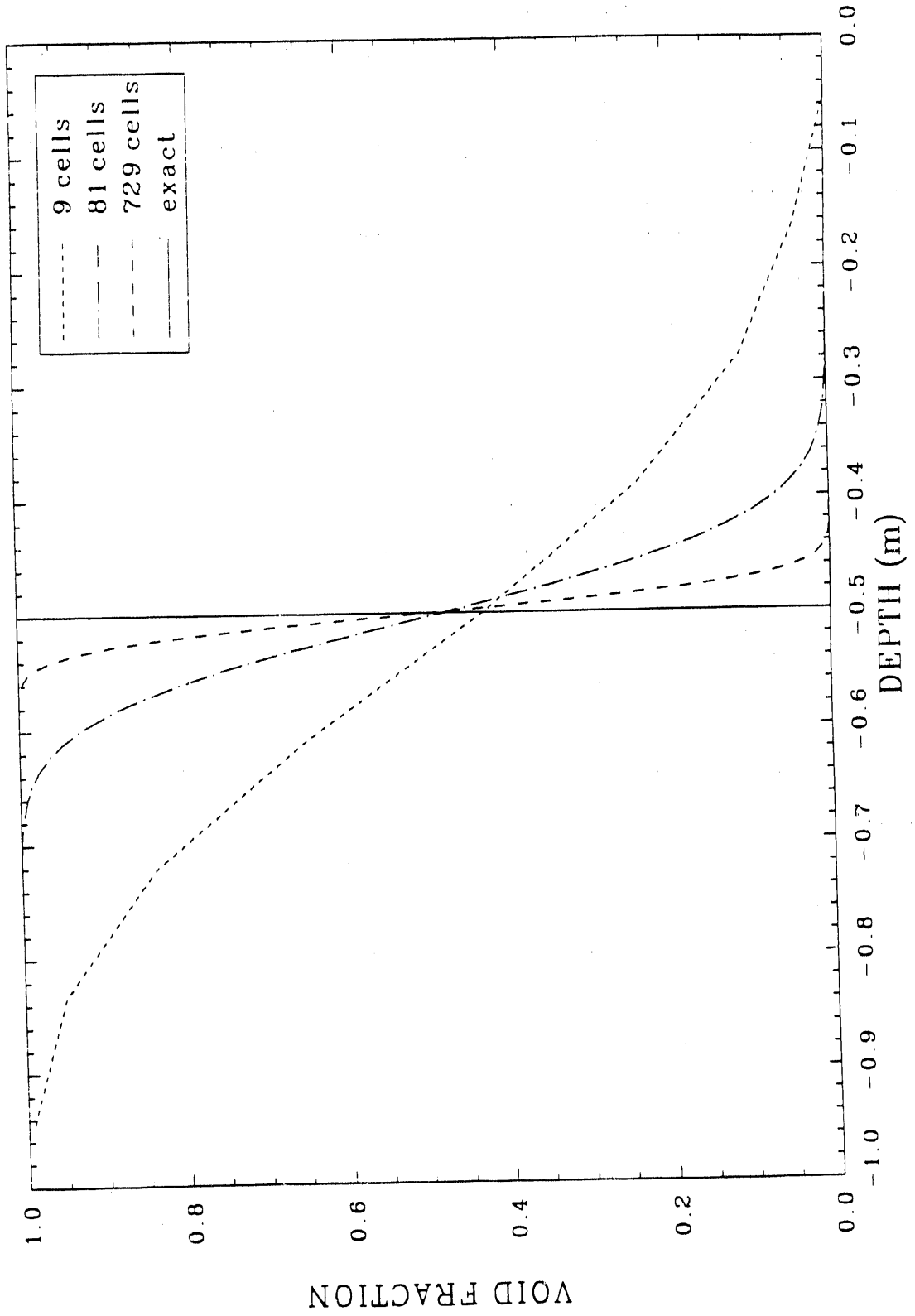
Table 4.1. Preliminary Comments about model Parameters

I. Materials Properties		
Parameter	Domain	Comments
gas density	0.5 - 50 kg/m <sup>3</sup>	represents H <sub>2</sub> to Xe at 1 atmosphere
liquid density	2 x 10 <sup>3</sup> - 2 x 10 <sup>4</sup> kg/m <sup>3</sup>	represents SiO <sub>2</sub> to U
interfacial surface tension	0.270 - 0.40 kg/s <sup>2</sup>	represents range of silicon melts reported in reference (Bikerman)
dynamic viscosity of liquid	.1 - 1000 kg/m-s	very large range

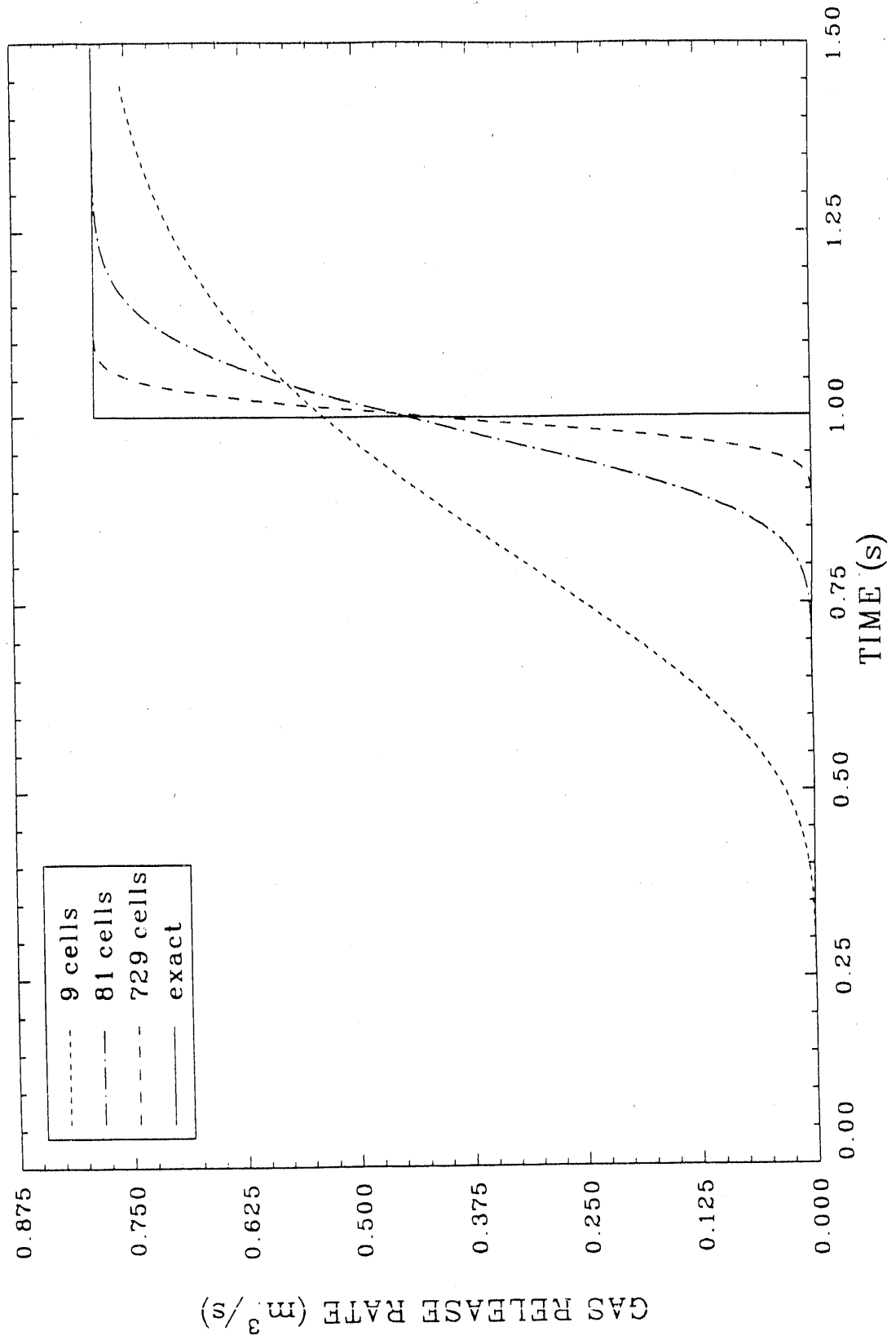
II. Boundary Conditions		
Parameter	Domain	Comments
initial bubble radius	to be determined	It is expected that this parameter will have to be determined by measurements with typical soils
gas source rates	10 <sup>-6</sup> - 1 kg/m <sup>2</sup> -s	The domain is large in order to include release from dry soils, evaporation of volatiles like water, lead, and cadmium, and pyrolysis.

Table 4.1. (continued)

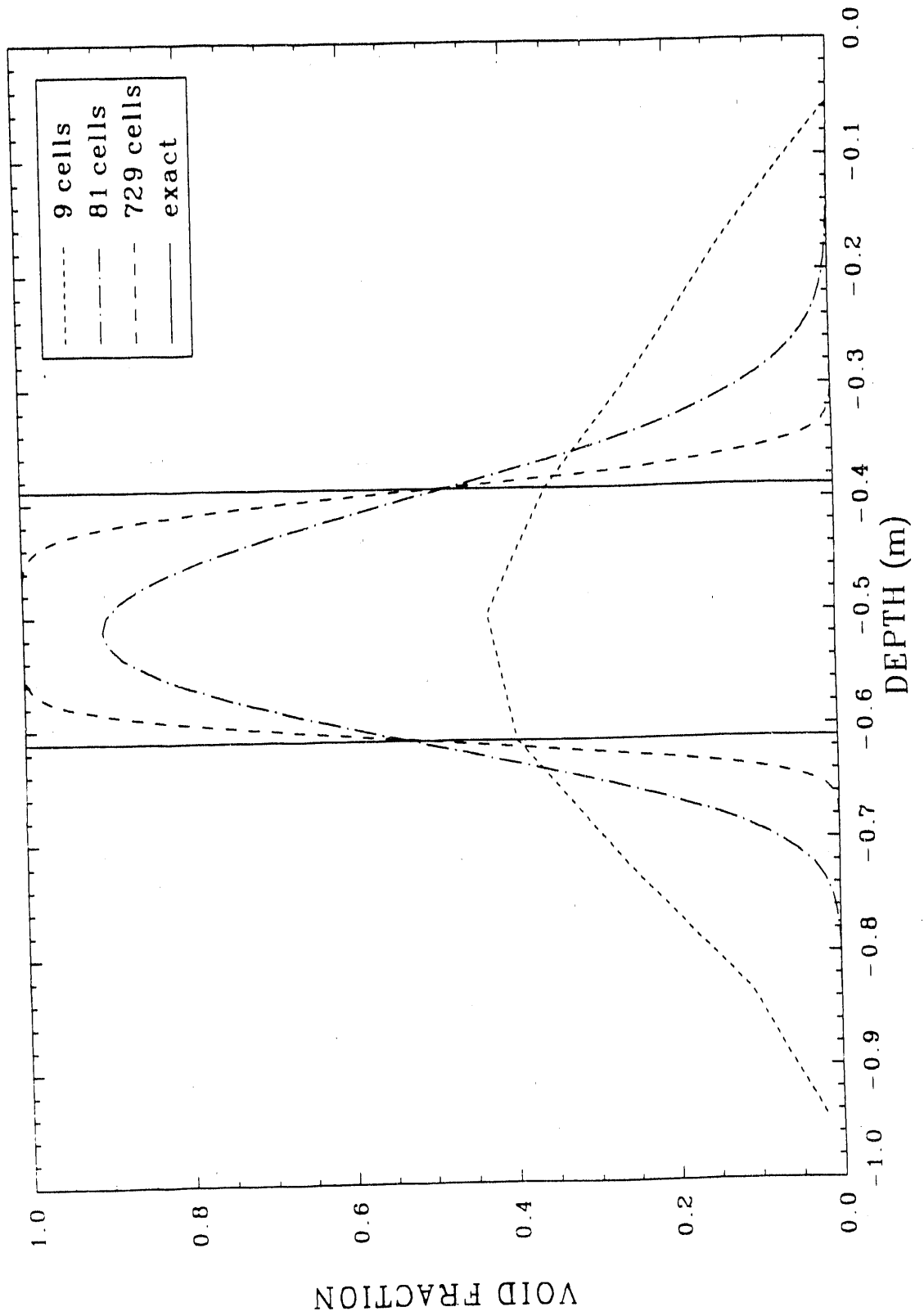
III. Model Assumptions		
Parameter	Domain	Comment
Terminal rise velocity versus size	to be determined	It is expected that this parameter will have to be confirmed by experiments in fluids similar to those modeled. The parametric study should help determine how accurate the experiments will need to be.
Agglomeration and breakup processes representations	to be determined	Some theoretical expressions are being developed using detailed models. These may have to be validated experimentally.



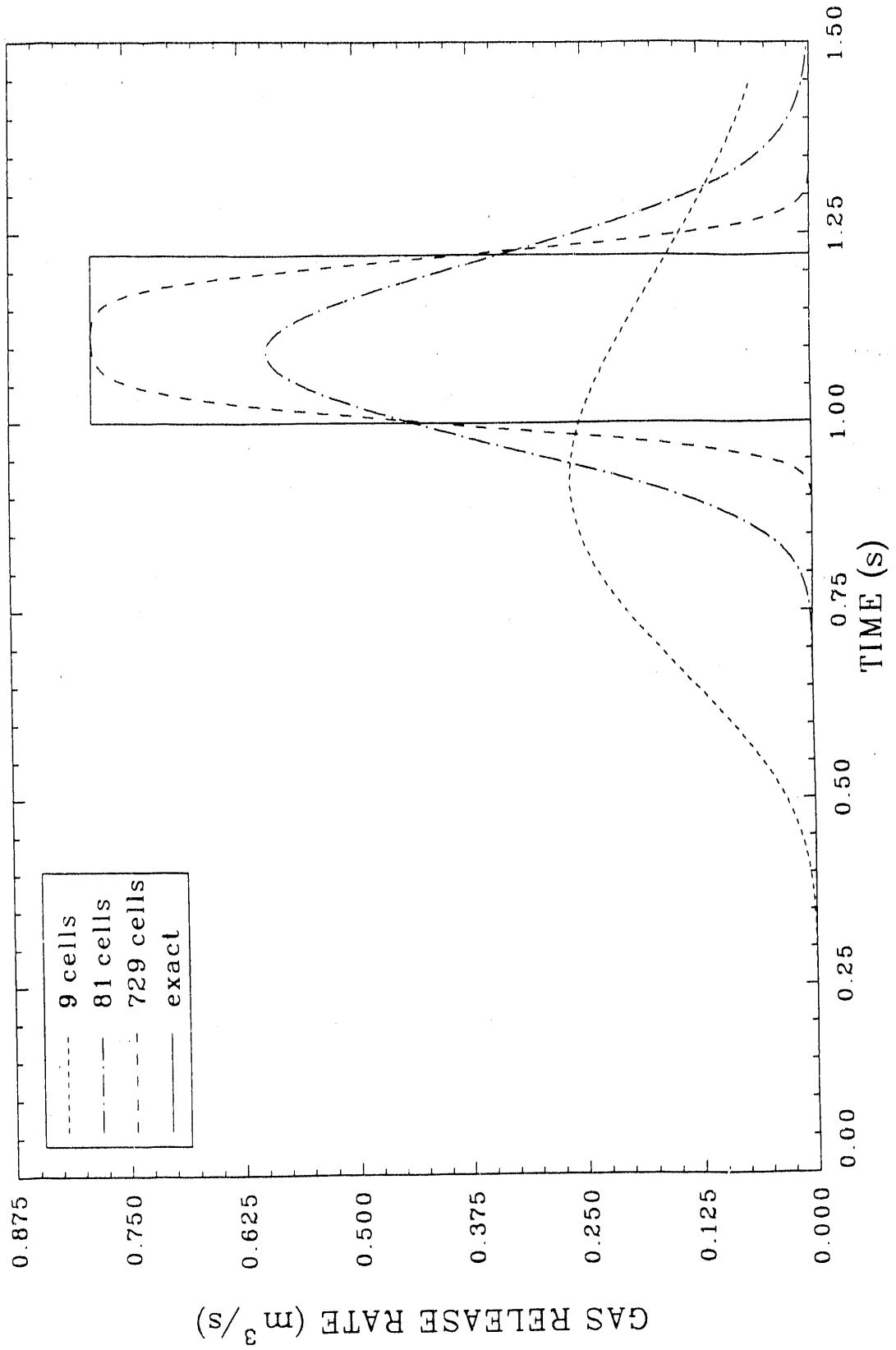
4.1 Spatial Distribution of Void Fraction at  $t = 0.5$  s for the Step Wave

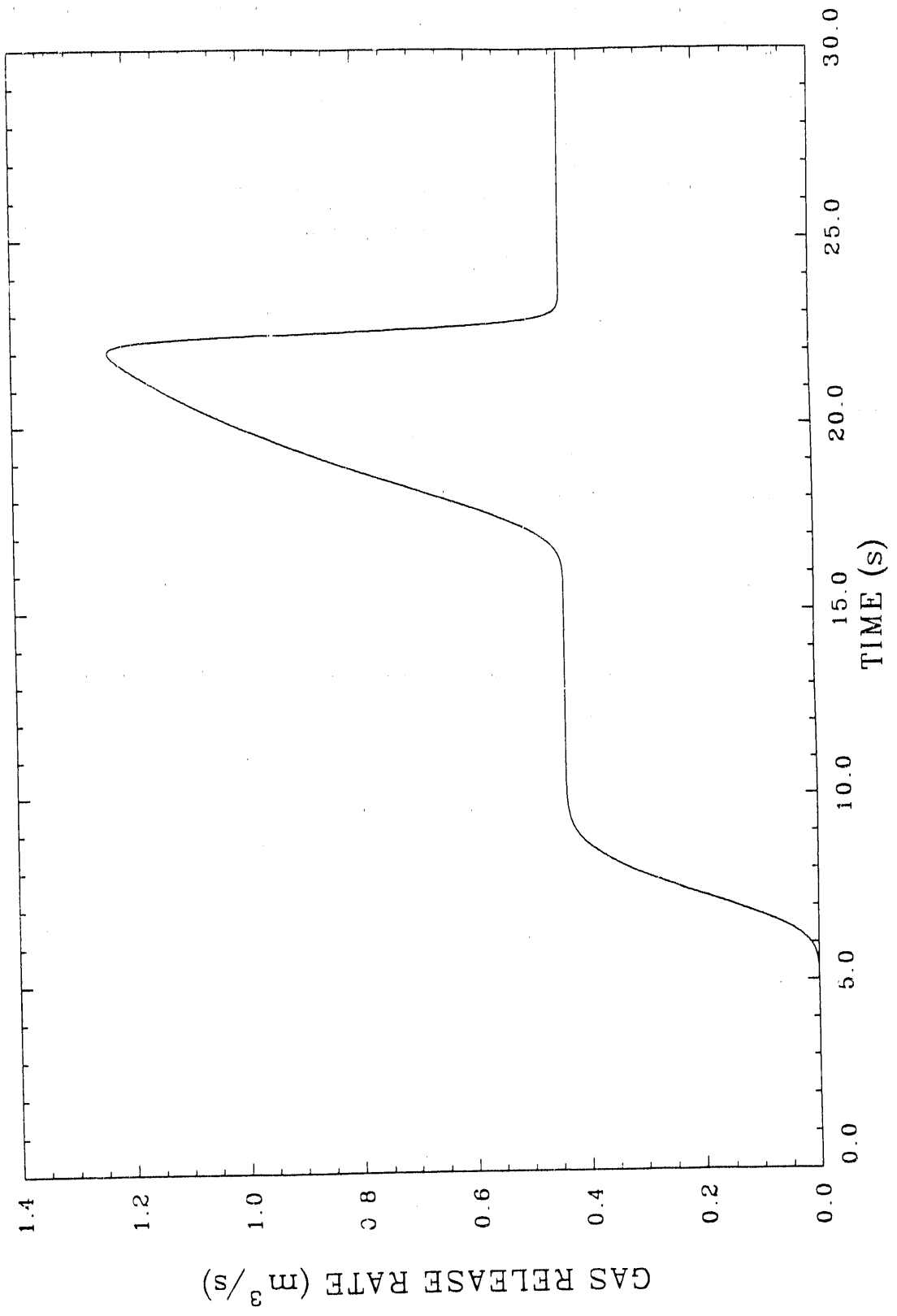


4.2 Gas Release vs. Time for Step Wave Propagation

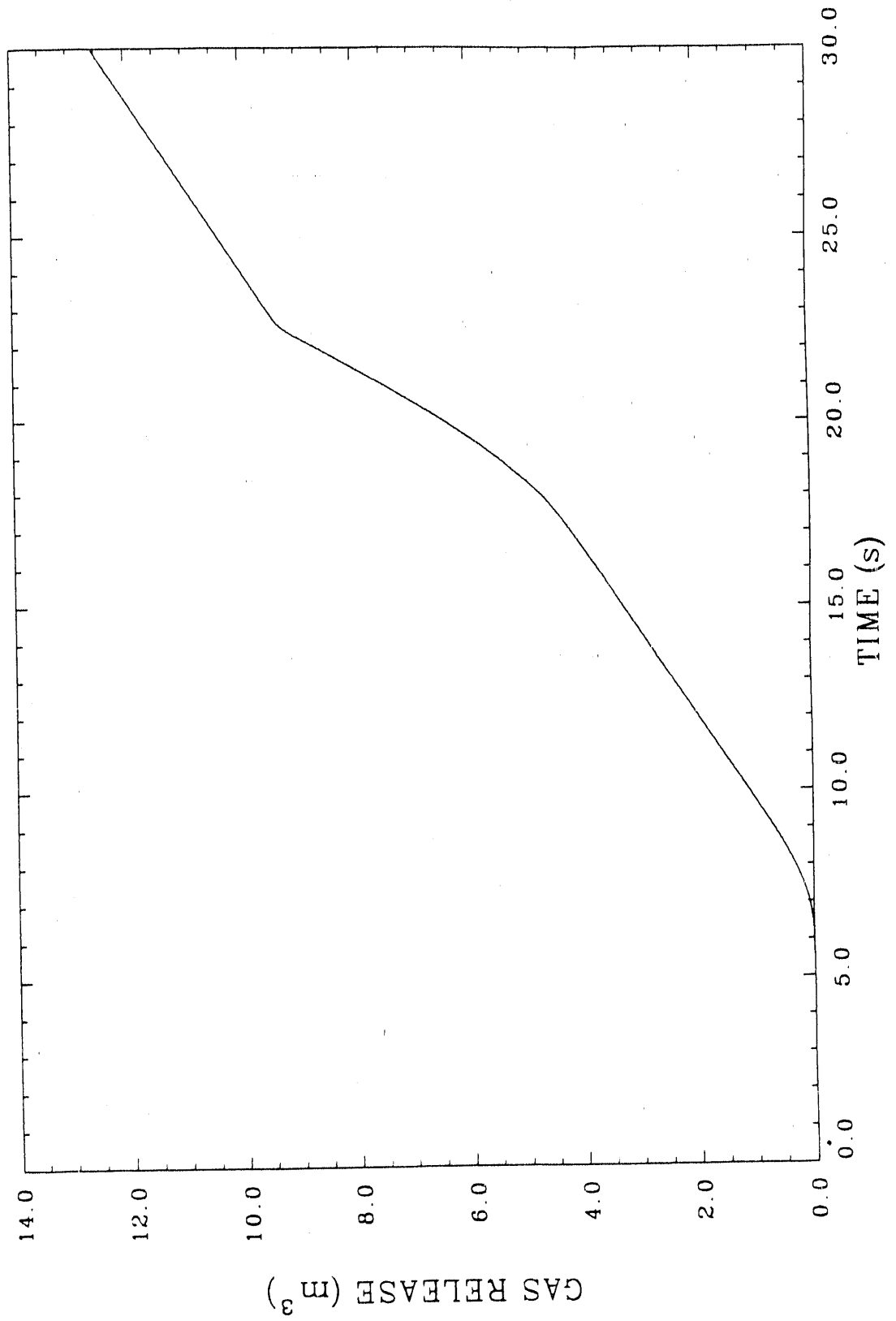


4.3 Spatial Distribution of Void Fraction at  $t = 0.61$  s for the Rectangular Wave





4.5 Off Gas Release Rate vs. Time for Combined Steady and Sudden Gas Influx



4.6 Total Gas Volume Released vs. Time for Combined Steady and Sudden Gas Influx



## REFERENCES

1. R. J. MacKinnon, P. E. Murray, et. al., In Situ Vitrification Model Development and Implementation Plan, EGG-WM-9036, EG&G Idaho, Inc., July 1990.
2. G. B. Wallis, One Dimensional Two-phase Flow, McGraw-Hill, New York, 1969.
3. F. N. Peebles and H. J. Garber, Studies on the Motion of Gas Bubbles in Liquids, Chemical Engineering Progress, Vol. 49, pp 88-97, 1953.
4. W. L. Haberman, and R. K. Morton, David W. Taylor Model Basin Rept. 802, 1953.
5. J. J. Bikerman, Surface Chemistry Theory and Applications, Academic Press Inc., New York, 1958.
6. M. Ishii and T. C. Chawla, Local Drag Laws in Dispersed Two-Phase Flow, NUREG/CR-1230, AND-79-105, 1979.
7. V. A. Mousseau and R. J. MacKinnon, Parametric Studies of Off-Gas Release During In Situ Vitrification, EG&G Idaho, Inc., to be published July 1990.
8. V. A. Mousseau and R. J. MacKinnon, In Situ Vitrification and Off-Gas Release Model Validation, EG&G Idaho, Inc., to be published September 1990.

APPENDIX

PROGRAM VARIABLE DICTIONARY

```

*comdeck dicton
c23456789012345678901234567890123456789012345678901234567890123456789012
c*****
c
c dictionary start
c
c*****
c
c sample entry
c
c varibl - ds - (kg,m,s,K,A) - description
c
c     d - derived
c     i - input
c     p - parameter or block data
c
c     s - scaler
c     v - vector
c
c     kg - kilograms
c     m - meters
c     s - second
c     K - degree Kelvin
c     A - Ampere
c
c
c
caaaaaaaaaaaaaaaaaaaaaaaaaaaaaaaaaaaaaaaaaaaaaaaaaaaaaaaaaaaaaaaaaaaaaaaaaa
c
c arhog - dv - (1,-3,0,0,0) - kg/(m**3) - The product of the void
c                                     fraction and the density of
c                                     the gas bubbles.
c arhogn - dv - (1,-3,0,0,0) - kg/(m**3) - The old time product of the
c                                     void fraction and the density
c                                     of the gas bubbles.
c
c
cbbbbbbbbbbbbbbbbbbbbbbbbbbbbbbbbbbbbbbbbbbbbbbbbbbbbbbbbbbbbbbbbbbbbbb
c
c bubnum - dv - (0,0,0,0,0) - no units - the number of average size
c                                     bubbles in a cell
c
c
cccccccccccccccccccccccccccccccccccccccccccccccccccccccccccccccccccccc
c
c cnvect - dv - (1,-3,-1,0,0) - kg/((m**3)*s) - the bubble convection
c                                     term in the continuity
c                                     equation.
c
c
cddddddddddddddddddddddddddddddddddddddddddddddddddddddddddddddddddddd
c
c debug - ps - (0,0,0,0,0) - no units - logical flag to turn on debug
c                                     output.
c depth - ds - (0,1,0,0,0) - m - depth of the melt pool.
c diamc - is - (0,1,0,0,0) - m - diameter of the cell.

```

```

c
c ccccccccccccccccccccccccccccccccccccccccccccccccccccccccccccccccccccccccccccccccccccccccccc
c
c epsgrv - ps - (0,1,-2,0,0) - m/(s**2) - the smallest acceleration do
c                                         to gravity before it is
c                                         considered zero.
c epsrad - pv - (0,1,0,0,0) - m - the radius that the bubble would be
c epsvb - ps - (0,1,-1,0,0) - m/s - the smallest bubble velocity before
c                                         it is considered zero.
c equrad - dv - (0,1,0,0,0) - m - the radius that the bubble would be
c                                         if it was spherical.
c
c ffffffffffffffffffffffffffffffffffffffffffffffffffffffffffffffffffffffffffffffffffffffffffffff
c
c four - ps - (0,0,0,0,0) - no units - the number four.
c
c ggggggggggggggggggggggggggggggggggggggggggggggggggggggggggggggggggggggggggggggggggggggggggg
c
c gamfirt - dv - (1,-3,-1,0,0) - kg/((m**3)*s) - added mass of bubbles
c                                         per volume of cell per
c                                         second at the melt
c                                         front.
c gamma - dv - (1,-3,-1,0,0) - kg/((m**3)*s) - added mass of bubbles
c                                         per volume of cell per
c                                         second.
c grav - is - (0,1,-2,0,0) - m/(s**2) - acceleration do to gravity.
c grwfirt - is - (0,0,0,0,0) - no units - the fraction that the bubble
c                                         size changes from top to
c                                         bottom due to agglomeration.
c
c hhhhhhhhhhhhhhhhhhhhhhhhhhhhhhhhhhhhhhhhhhhhhhhhhhhhhhhhhhhhhhhhhhhhhhhhhhhhhhhhhhhhhhhhhhh
c
c half - ps - (0,0,0,0,0) - no units - the fraction one half.
c height - ds - (0,1,0,0,0) - m - the depth below ground.
c
c kkkkkkkkkkkkkkkkkkkkkkkkkkkkkkkkkkkkkkkkkkkkkkkkkkkkkkkkkkkkkkkkkkkkkkkkkkkkkkkkkkkkkkkkkkk
c
c k - ds - (0,0,0,0,0) - no units - do loop index for volume loops.
c kk - ds - (0,0,0,0,0) - no units - do loop index for volume loops
c                                         when a second one is needed.
c
c
c llllllllllllllllllllllllllllllllllllllllllllllllllllllllllllllllllllllllllllllllllllllllllll
c
c lowact - ds - (0,0,0,0,0) - no units - the lowest active cell. This
c                                         determines where the melt front
c                                         is located.
c lwact0 - is - (0,0,0,0,0) - no units - the lowest active cell
c                                         initially.
c
c
c ttttttttttttttttttttttttttttttttttttttttttttttttttttttttttttttttttttttttttttttttttttttttttttt
c
c maxcyc - is - (0,0,0,0,0) - no units - maximum number of cycles.

```

```

c
c ccccccccccccccccccccccccccccccccccccccccccccccccccccccccccccccccccccccccccccccccc
c
c nbub0 - is - (0,0,0,0,0) - no units - flag for bubble initialization
c                                     (1) - uniform at pore size
c                                     (0) - gradient due to density
c nbug - ps - (0,0,0,0,0) - no units - unit number for debug output.
c nc - ps - (0,0,0,0,0) - no units - maximum number of cycles.
c ncelin - is - (0,0,0,0,0) - no units - cell number to inject bubbles
c                                     into the flow.
c ncells - is - (0,0,0,0,0) - no units - number of active cells in model
c nclskp - is - (0,0,0,0,0) - no units - number of cells to skip for
c                                     surface output.
c ncp1 - is - (0,0,0,0,0) - no units - number active of cells in model
c                                     plus one.
c ncp2 - is - (0,0,0,0,0) - no units - number active of cells in model
c                                     plus two.
c ncvbss - is - (0,0,0,0,0) - no units - flag for computing the steady
c                                     state bubble velocity
c                                     (1) - compute using wallis
c                                     (0) - use vbinp that is
c                                     read in.
c ncyc - ds - (0,0,0,0,0) - no units - current number of time steps.
c ncycft - is - (0,0,0,0,0) - no units - the number of cycles it takes
c                                     to move the melt front one
c                                     cell forward.
c ncyacin - is - (0,0,0,0,0) - no units - the cycle number to inject
c                                     voidin amount of void in
c                                     cell ncelin.
c ncyacsb - is - (0,0,0,0,0) - no units - the number of cycles it takes
c                                     to move the surface one
c                                     cell down.
c ndbstp - is - (0,0,0,0,0) - no units - cycle number to stop debug
c                                     output.
c ndbstt - is - (0,0,0,0,0) - no units - cycle number to start debug
c                                     output.
c ngrf1 - ps - (0,0,0,0,0) - no units - unit number for time dependant
c                                     graphics output.
c ngrf2 - ps - (0,0,0,0,0) - no units - unit number for surface
c                                     graphics output.
c nhiact - ds - (0,0,0,0,0) - no units - the highest active cell. This
c                                     determines where the surface
c                                     is located.
c nhiac0 - is - (0,0,0,0,0) - no units - the highest active cell
c                                     initially.
c nin - ps - (0,0,0,0,0) - no units - unit number for input.
c norfis - ps - (0,0,0,0,0) - no units - flag for bottom bubble size
c                                     (1) computed
c                                     (0) input value radbt0
c nout - ps - (0,0,0,0,0) - no units - unit number for output.
c nplot - is - (0,0,0,0,0) - no units - number of cycles between
c                                     plotting output.
c

```



```

c
c sigf0 - is - (1,0,-2,0,0) - kg/(s**2) - The reference surface tension
c sigmaf - dv - (1,0,-2,0,0) - kg/(s**2) - The surface tension of the
c
c cells.
c
c
c tttttttttttttttttttttttttttttttttttttttttttttttttttttttttttttttttt
c
c t0 - is - (0,0,0,1,0) - K - The reference temperature.
c three - ps - (0,0,0,0,0) - no units - the number three.
c timcon - is - (0,0,1,0,0) - s - the time it takes for a bubble to
c
c change size.
c time - ds - (0,0,1,0,0) - s - the simulation time.
c temp - dv - (0,0,0,1,0) - K - The temperature of the melt in a cell.
c
c
c vvvvvvvvvvvvvvvvvvvvvvvvvvvvvvvvvvvvvvvvvvvvvvvvvvvvvvvvvvvvvvvvvv
c
c vb - dv - (0,1,-1,0,0) - m/s - the velocity of the bubble.
c vbbc - is - (0,1,-1,0,0) - m/s - the flux boundary bubble velocity.
c vbinp - is - (0,1,-1,0,0) - m/s - input terminal velocity of the
c
c bubble to be used if gravity is
c zero or ncvbss equals zero.
c vbn - dv - (0,1,-1,0,0) - m/s - the old time velocity of the bubble
c vbss - dv - (0,1,-1,0,0) - m/s - the steady state velocity of the
c
c bubble.
c vbss0 - dv - (0,1,-1,0,0) - m/s - the initial steady state velocity
c
c of the bubble.
c vbssn - dv - (0,1,-1,0,0) - m/s - the old time steady state velocity
c
c of the bubble.
c viscf - dv - (1,-1,-1,0,0) - kg/(m*s) - the viscosity of the melt in
c
c the cell.
c viscf0 - dv - (1,-1,-1,0,0) - kg/(m*s) - the reference viscosity of
c
c the melt.
c vmelt - is - (0,1,-1,0,0) - m/s - the vertical velocity of the melt
c
c pool.
c void - dv - (0,0,0,0,0) - no units - the vapor volume fraction.
c void0 - is - (0,0,0,0,0) - no units - initial void fraction.
c voidbc - is - (0,0,0,0,0) - no units - the flux boundary void fraction
c voidin - dv - (0,0,0,0,0) - no units - amount of void to inject
c
c into the flow.
c voidn - dv - (0,0,0,0,0) - no units - old time vapor volume fraction.
c volb0 - is - (0,3,0,0,0) - m**3 - the reference volume of the
c
c average bubble.
c volbot - ds - (0,3,0,0,0) - m**3 - the volume of the bubbles at the
c
c melt front.
c volb - dv - (0,3,0,0,0) - m**3 - the volume of the average bubble
c
c in a cell.
c volbn - dv - (0,3,0,0,0) - m**3 - the old time volume of the average
c
c bubble in a cell.
c volcel - ds - (0,3,0,0,0) - m**3 - volume of the cell assuming a
c
c cylindrical geometry.
c voltop - ds - (0,3,0,0,0) - m**3 - the volume of the bubbles at the
c
c top of the melt.

```

```
C
C*****
C
C wate - ds - (0,0,0,0,0) - no units - the under-relaxation to keep
C the bubbles from changing
C volume too rapidly.
C wecrit - ds - (0,0,0,0,0) - no units - the critical weber number
C which determines when bubbles
C break-up.
C
CXXXXXXXXXXXXXXXXXXXXXXXXXXXXXXXXXXXXXXXXXXXXXXXXXXXXXXXXXXXXXXXXXXXX
C
C xk - dv - (0,1,0,0,0) - m - the cell center location.
C
CZZZZZZZZZZZZZZZZZZZZZZZZZZZZZZZZZZZZZZZZZZZZZZZZZZZZZZZZZZZZZZZZZZ
C
C zero - ps - (0,0,0,0,0) - no units - the number zero.
C
C*****
C
C dictionary end
C
C*****
```



**END**

**DATE FILMED**

12 / 10 / 90

